

Synthesis of Novel c(AmpRGD)-Sunitinib Dual Conjugates as Molecular Tools Targeting the $\alpha_5\beta_1$ Integrin/VEGFR2 Couple and Impairing Tumor-Associated Angiogenesis

Andrea Sartori, Elisabetta Portioli, Lucia Battistini, Lido Calorini, Alberto Pupi, Federica Vacondio, Daniela Arosio, Francesca Bianchini, and Franca Zanardi

J. Med. Chem., **Just Accepted Manuscript** • DOI: 10.1021/acs.jmedchem.6b01266 • Publication Date (Web): 06 Dec 2016

Downloaded from <http://pubs.acs.org> on December 6, 2016

Just Accepted

“Just Accepted” manuscripts have been peer-reviewed and accepted for publication. They are posted online prior to technical editing, formatting for publication and author proofing. The American Chemical Society provides “Just Accepted” as a free service to the research community to expedite the dissemination of scientific material as soon as possible after acceptance. “Just Accepted” manuscripts appear in full in PDF format accompanied by an HTML abstract. “Just Accepted” manuscripts have been fully peer reviewed, but should not be considered the official version of record. They are accessible to all readers and citable by the Digital Object Identifier (DOI®). “Just Accepted” is an optional service offered to authors. Therefore, the “Just Accepted” Web site may not include all articles that will be published in the journal. After a manuscript is technically edited and formatted, it will be removed from the “Just Accepted” Web site and published as an ASAP article. Note that technical editing may introduce minor changes to the manuscript text and/or graphics which could affect content, and all legal disclaimers and ethical guidelines that apply to the journal pertain. ACS cannot be held responsible for errors or consequences arising from the use of information contained in these “Just Accepted” manuscripts.

1
2
3
4
5
6
7
8
9
10
11
12
13
14
15
16
17
18
19
20
21
22
23
24
25
26
27
28
29
30
31
32
33
34
35
36
37
38
39
40
41
42
43
44
45
46
47
48
49
50
51
52
53
54
55
56
57
58
59
60

Synthesis of Novel c(AmpRGD)-Sunitinib Dual Conjugates as Molecular Tools Targeting the $\alpha_v\beta_3$ Integrin/VEGFR2 Couple and Impairing Tumor- Associated Angiogenesis

Andrea Sartori,^[a] Elisabetta Portioli,^[a] Lucia Battistini,^[a] Lido Calorini,^[b] Alberto Pupi,^[b,c]

Federica Vacondio,^[a] Daniela Arosio,^[d] Francesca Bianchini,^{[b,c]} and Franca Zanardi^{*[a]}*

[a] Dipartimento di Farmacia, Università degli Studi di Parma, Parco Area delle Scienze 27A,
43124 Parma, Italy

[b] Dipartimento di Scienze Biomediche, Sperimentali e Cliniche “Mario Serio”, Università
degli Studi di Firenze, Viale G. B. Morgagni 50, 50134 Firenze, Italy

[c] Centro Interdipartimentale per lo Sviluppo Preclinico dell’Imaging Molecolare (CISPIM),
Università degli Studi di Firenze, Viale G. B. Morgagni 50, 50134 Firenze, Italy

[d] Istituto di Scienze e Tecnologie Molecolari, Consiglio Nazionale delle Ricerche, Via Golgi
19, 20133 Milano, Italy

KEYWORDS: Angiogenesis, Dual conjugates, Growth Factor Receptors, Integrins, RGD
Ligands, Peptidomimetics, Sunitinib

ABSTRACT

Based on a previously discovered anti- $\alpha_v\beta_3$ integrin peptidomimetic – c(AmpRGD) – and the clinically approved anti-angiogenic kinase inhibitor sunitinib, three novel dual conjugates were synthesized (compounds **1-3**), featuring the covalent and robust linkage between these two active modules. In all conjugates, the ligand binding competence toward $\alpha_v\beta_3$ (using both isolated receptors and $\alpha_v\beta_3$ -overexpressing endothelial progenitor EP cells) and the kinase inhibitory activity (toward both isolated kinases and EPCs) remained almost untouched and comparable to the activity of the single active units. Compounds **1-3** showed interesting anti-angiogenesis properties in an in vitro tubulogenic assay; furthermore, dimeric-RGD conjugate **3** strongly inhibited in vivo angiogenesis in Matrigel plug assays in FVB mice. These results offer proof-of-concept of how the covalent conjugation of two angiogenesis-related small modules may result in novel and stable molecules, which impair tumor-related angiogenesis with equal or even superior ability as compared to the single modules or their simple combinations.

INTRODUCTION

Targeted therapy that selectively addresses oncogenic drivers,¹⁻³ as well as the use of drugs concomitantly perturbing multiple molecular targets and signaling pathways⁴⁻⁶ are arising as privileged therapeutic options. Angiogenesis, the process by which new blood vessels arise from preexisting vasculature, plays crucial roles in both normal and pathological events. In particular, aberrant angiogenesis – involving constantly activated vasculature – is widely accepted as a key player in a variety of pathological conditions including cancer growth and metastasis,

1
2
3 rheumatoid arthritis and age-related macular degeneration. Many diverse endogenous molecular
4 systems participate in the angiogenesis regulation, including pro-angiogenic vascular endothelial
5 growth factors (VEGFs), platelet-derived growth factors (PDGFs), their associated tyrosine
6 kinase receptors (VEGFRs and PDGFRs), matrix metalloproteinases (MMPs), ephrin-ephrin
7 receptor complexes, and specific extracellular matrix (ECM)-recognizing integrin receptors as
8 $\alpha_V\beta_3$, $\alpha_V\beta_5$ and $\alpha_5\beta_1$.⁷⁻¹²
9
10
11
12
13
14
15
16

17
18 Substantial four decade-long body of research in this field resulted in worldwide approval by
19 drug agencies of effective anti-angiogenic drugs including the humanized monoclonal antibodies
20 trastuzumab and bevacizumab, which are VEGF antagonists, and several small molecules such
21 as sunitinib and sorafenib, which mainly target the highly conserved cytosolic tyrosine kinase
22 domain of VEGFRs.^{9,12} Sunitinib, in particular (Figure 1), is an alkylidene 2-oxindole agent
23 which acts as a highly effective multitarget tyrosine kinase inhibitor (TKI, mainly against
24 VEGFR2, PDGFR β , cKit, and Flt-3),¹³⁻¹⁶ it is indicated as first-line therapy for metastatic renal
25 cell carcinoma, pancreatic neuroendocrine tumors, second-line therapy for imatinib-resistant
26 gastrointestinal stromal tumors,¹³⁻¹⁶ and it is still the focus of countless clinical trials.¹⁷
27
28
29
30
31
32
33
34
35
36
37
38
39
40

41 Among antiangiogenic $\alpha_V\beta_3$ -integrin inhibitors, the small molecule cilengitide [c(RGD)NMefV]
42 is the most widely studied, and several advanced clinical trials are still in progress concerning the
43 use of this drug as either single agent or in combination with radiotherapy.¹⁸⁻²¹ However, the
44 limited long-term efficacy and the systemic toxicity associated with the clinical use of the
45 approved anti-angiogenic drugs posed serious concerns about the actual benefit and safety of
46 these treatments.²²⁻²⁹
47
48
49
50
51
52
53
54
55
56
57
58
59
60

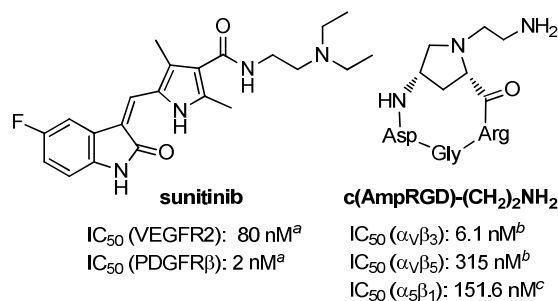


Figure 1. The antiangiogenic drug sunitinib and the 4-aminoproline-based RGD cyclotetrapeptide c(AmpRGD)-(CH₂)₂NH₂. ^aRef. 13; ^bRef. 42; ^cRef. 43.

While the debate about the actual usefulness of anti-angiogenesis therapy remains open,²²⁻²⁹ current researches suggest that possible solutions could entail the use of drugs capable of hitting multiple targets/pathways and cell types involved in the tumor microenvironment,^{10,12,25,29,30} while possessing supplemental selective targeting moieties.

Among the intricate, often overlapping cell signaling networks regulating angiogenesis, growing evidence emerged for strict crosstalk between the VEGFR2 and α_vβ₃ receptors.³¹⁻³⁶ These two receptors are physically and functionally connected in common cell populations (e.g. endothelial cells, ECs, and several cancer cell types) and their interactions are important for both integrin activation and mutual regulation of the kinase activity.³¹⁻³⁶ Blockage of the α_vβ₃/VEGFR2 couple may thus be of high therapeutic potential.³⁷⁻⁴⁰ In fact, the combined use of two small molecules – cilengitide and the sunitinib analogue SU5416 (Figure 2, A) – showed anti-angiogenic effect and inhibition of tumor melanoma growth and metastasis during in vivo preclinical studies.³⁷ In this instance, however, the two drugs were independently delivered, with possible differences in localization and pharmacokinetics. In an enlightening study,³⁸ a dual

specific scVEGF protein was engineered, capable of binding the extracellular portions of $\alpha_v\beta_3$ and VEGFR2 simultaneously, showing promise for effective in vitro and in vivo anti-angiogenic action (Figure 2, B). Though highly promising, this work had the limitation of dealing with complex engineered 25 kDa-weighty proteins.

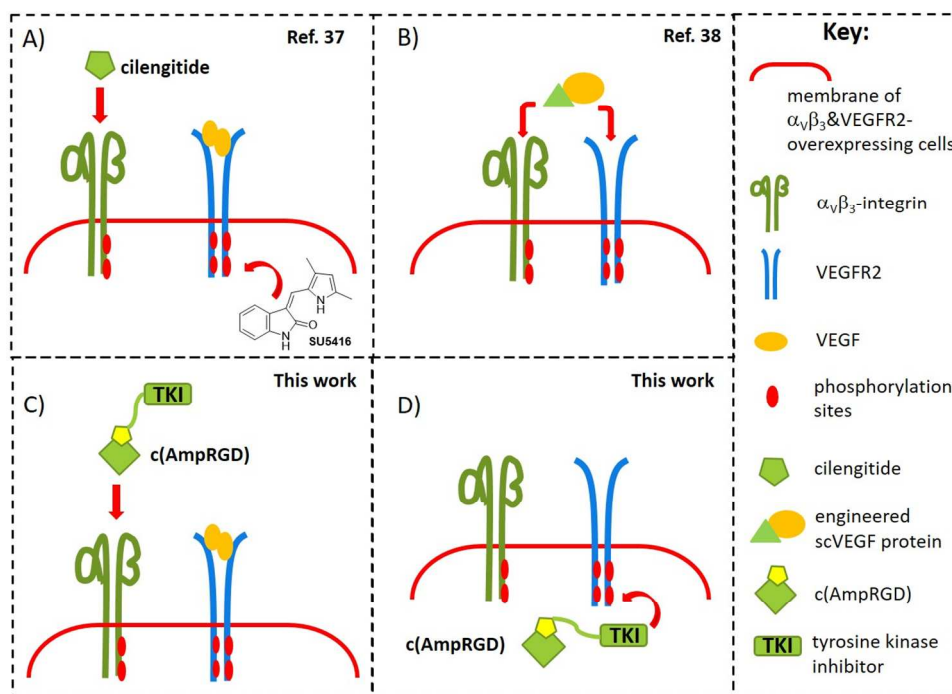


Figure 2. A) $\alpha_v\beta_3$ antagonist cilengitide (outside cell)+VEGFR2 antagonist (inside), two discrete small molecules, different localization (Ref. 37); B) one engineered dual-specific protein (outside), simultaneous $\alpha_v\beta_3$ /VEGFR2 inhibition (Ref. 38); C) and D) one small molecule, the c(AmpRGD)-TKI conjugate, recognizing $\alpha_v\beta_3$ (outside), partially entering the cell (possibly via $\alpha_v\beta_3$), and antagonizing VEGFR2 (inside) (this work).

1
2
3 A complementary and conceptually different approach is here proposed, according to which a
4 selective binder of the extracellular segment of $\alpha_v\beta_3$ is covalently linked to a proven TKI such as
5 sunitinib, whose interaction with the cytoplasmic domain of VEGFR2 is widely recognized. As
6 $\alpha_v\beta_3$ binder, we could rely on a recently discovered series of aminoproline-based RGD
7 cyclotetrapeptides of type $c(\text{AmpRGD})-(\text{CH}_2)_2\text{NH}_2$ (Figure 1)⁴¹⁻⁴³ which showed remarkable and
8 selective binding capability toward the $\alpha_v\beta_3$ integrin receptor in both cell-free and cell assays.
9
10 The covalent assemblage of an anchorable sunitinib-like moiety to the $c(\text{AmpRGD})$ portion
11 through a suitable linker would furnish dual conjugates (Figure 2 C and 2 D, schematic
12 representation) wherein the RGD unit would possibly provide *i*) EC-selective targeting by $\alpha_v\beta_3$ -
13 RGD recognition, *ii*) $\alpha_v\beta_3$ -dependent anti-angiogenic effect, and *iii*) $\alpha_v\beta_3$ -mediated cell
14 internalization. On the other hand, the sunitinib unit could exert its intracellular TKI effect after
15 internalization, while playing a role in overall perturbation of the $\alpha_v\beta_3$ -VEGFR2 crosstalk.⁴⁴⁻⁴⁶
16
17

18
19 We herein disclose the design, synthesis, and biological activity evaluation of three novel
20 covalent prototypes **1-3** (Figure 3). In particular, the binding properties toward $\alpha_v\beta_3$ integrin,
21 kinase inhibitory activity, cell uptake, and anti-angiogenesis potential in vitro and in vivo are
22 reported and discussed, vis-à-vis the behavior of the single modules and their simple
23 combinations.
24
25
26
27
28
29
30
31
32
33

34 RESULTS AND DISCUSSION

35
36
37
38
39
40
41
42
43
44
45
46
47
48
49
50
51
52
53
54 **Design of cAmpRGD-sunitinib Conjugates.** To fulfill the objectives of this work (Figure 2 C
55 and 2 D), the projected dual conjugates had to embody several stringent requisites. First, *the*
56
57
58
59
60

1
2
3 *active units should not disturb each other*, that is, the sunitinib moiety should not compromise
4 the RGD-binding capability while the RGD unit should not impede the tyrosine kinase activity of
5 sunitinib. Second, to *exclude premature detachment* of the two active units (outside the targeted
6 cells), the linker between them should be either uncleavable or cleaved within cells exclusively;
7 and third, *the conjugate must enter the targeted cells* possibly via $\alpha_V\beta_3$ -mediated endocytosis.
8
9

10
11
12
13
14
15
16 As a background, extensive structure-activity relationship studies on sunitinib analogues^{13,47} and
17 X-ray analysis of the complex between the drug and the tyrosine kinase domain of the VEGFR2
18 active site^{48,49} revealed that the aromatic portion of the molecule is directly involved in the
19 binding, while the terminal tertiary amine stands outside the pocket and may allow certain
20 margins of structural modifications. Thus, connection of sunitinib to the linker exploiting this
21 amine terminal would likely be uninfluential toward the tyrosine kinase activity. Furthermore,
22 we were aware of the binding capability and selectivity toward the $\alpha_V\beta_3$ integrin of
23 c(AmpRGD)-based ligands and related conjugates,^{41-43,50,51} anticipating that conjugation of these
24 ligands with the ancillary sunitinib moiety would not hardly compromise their $\alpha_V\beta_3$ -integrin
25 binding ability. Lastly, the cell internalization potential of c(AmpRGD)-conjugates was
26 preliminarily assayed using a c(AmpRGD)-fluorescein conjugate control which demonstrated
27 complete $\alpha_V\beta_3$ -dependent internalization in A375 melanoma cells within 25 min exposure (see
28 details in the Supporting Information).
29
30
31
32
33
34
35
36
37
38
39
40
41
42
43
44
45
46
47
48
49
50
51
52
53
54
55
56
57
58
59
60

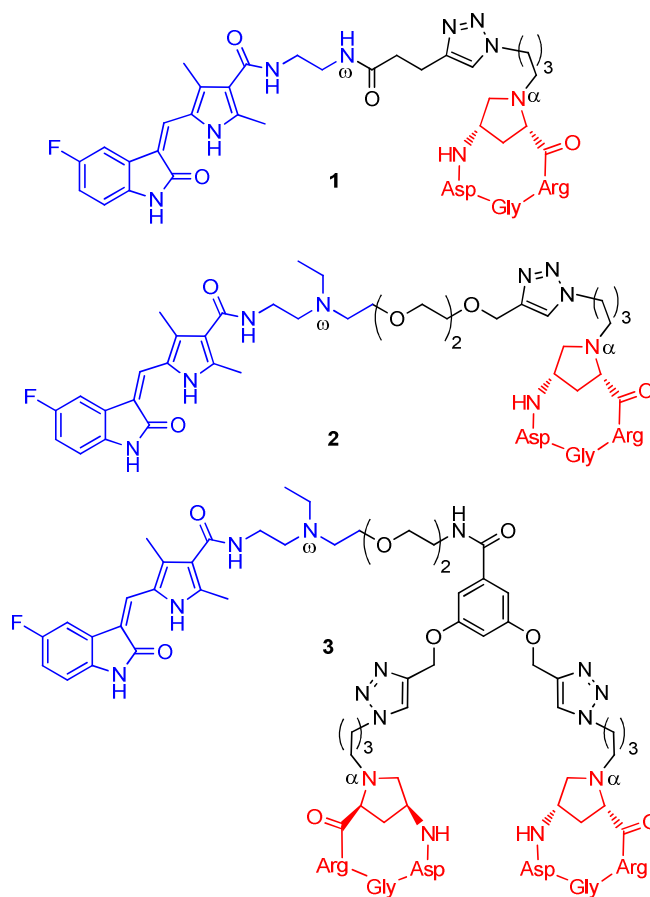
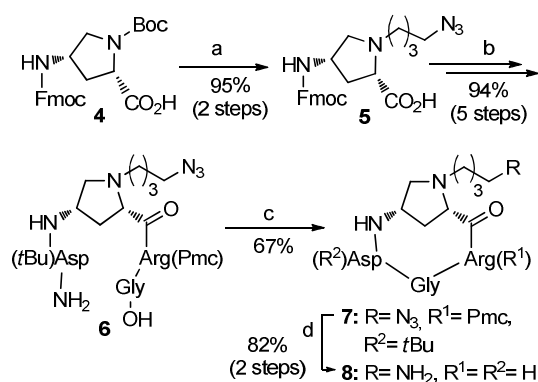


Figure 3. Structure of the targeted dual conjugates **1-3**.

With these clues at hand, conjugates **1-3** were designed, wherein the two active units are positioned 11-to-22 bonds away (Figure 3, N^α to N^ω) and are connected via robust triazole/ether/amide linkages, as shown in Figure 3. Monomeric compounds **1** and **2** differ from each other in the linker length and type; compounds **2** and **3** share a common pegylated linker and maintain the tertiary amine functionality of the parent drug, while compound **1** replaces this amine with a secondary amide. Finally, compound **3** features a dimeric RGD presentation, which could be important for enhanced integrin recognition and integrin-mediated cell internalization.⁵²⁻⁵⁷

Chemistry. The synthesis began with the preparation of three constitutive modules namely, the c(AmpRGD)-azide **7** (Scheme 1), the sunitinib analogue **13** (Scheme 2), and the linker moieties **14**, **16**, and **18** (Scheme 3 and Supporting Information). Thus, commercially available protected *cis*-amino-L-proline **4** was selectively deprotected at the *N*(α)-site and alkylated via reductive amination using 4-azidopropanal (Scheme 1).

Scheme 1. Synthesis of the c(AmpRGD) Modules **7** and **8**^a

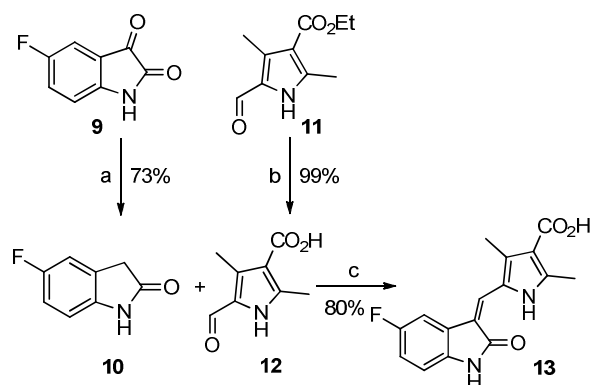


^aReagents and conditions: (a) (i) TFA, DCM, rt; (ii) 4-azidobutanal, NaBH(OAc)₃, 1,2-DCE, rt; (b) *Fmoc-SPPS*: (i) Cl-cTrt-O-Gly-(Pmc)Arg-NH₂, **5**, HATU, HOAt, collidine, DMF, rt; (ii) piperidine, DMF, rt; (iii) Fmoc-Asp(*t*BuO)-OH, HATU, HOAt, collidine, DMF, rt; (iv) piperidine, DMF, rt; (v) AcOH, TFE, DCM, rt; (c) HATU, HOAt, collidine, DCM/DMF, rt; (d) (i) H₂, Pd/C, EtOH, rt; (ii) TFA/TIS/H₂O (95:2.5:2.5), rt.

Azidoproline **5** was efficiently obtained (95% yield), and inserted into the projected peptide chain via conventional Fmoc-based solid phase peptide synthesis (Fmoc-SPPS) using chlorotrityl (cTrt) resin. After detachment from the resin, **6** was recovered in 94% yield and subjected to in-solution cyclization under diluted conditions (13:1 DCM/DMF solvent mixture, 2.2 mM), using

1
2
3 the HATU/HOAt reagent couple, giving protected azido-terminating cyclotetrapeptide **7**, ready
4
5 for the subsequent conjugation step. Overall, the novel azide module **7** was prepared in a eight-
6
7 step sequence and rewarding 63% overall yield from proline **4**. Azide **7** could be also
8
9 conveniently converted to free amine **8** via reduction and acidic deprotection (82%, two steps),
10
11 which served as a reference control during the biological assays (vide infra). It is to be noted that
12
13 the synthesis of similar c(AmpRGD) azide/amine congeners possessing two carbon-long alkyl
14
15 chains instead of four was reported by us in previous works;^{42,43} in that instances, however,
16
17 longer linear sequences were experienced (14-15 steps) and lower yields were obtained (10-16%
18
19 overall yields).

25 26 Scheme 2. Synthesis of the Sunitinib-Like Module 13^a



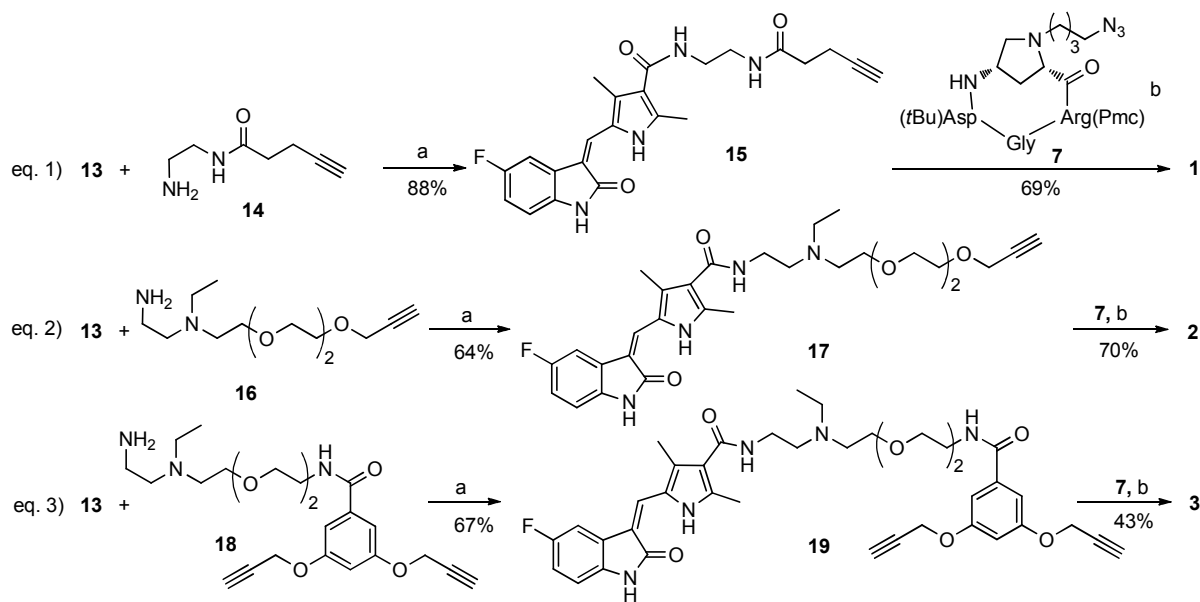
43 ^aReagents and conditions: (a) NH₂NH₂, 100 °C; (b) KOH, H₂O, MeOH, reflux; (c) piperidine,
44
45 EtOH, 60 °C.

46
47
48
49
50
51
52 As for the sunitinib portion, carboxylic acid **13** was judged a good precursor. As shown in
53
54 Scheme 2, Knoevenagel condensation between oxindole **10**, in turn obtained from commercial 5-
55
56 fluoroisatin **9** by Wolff-Kishner reduction, and pyrrole acid **12** (from saponification of the
57
58
59
60

1
2
3 corresponding commercial ethyl ester **11**) consigned 3-alkylidene 2-oxindole **13** in a good 80%
4
5 yield,¹³ as the sole detectable *Z*-configured isomer.⁵⁸
6
7

8
9 Simple chemistry was used to access alkyne-terminating amine **14**, pegylated counterpart **16**, and
10
11 bis-alkyne amine **18** (structures in Scheme 3), whose straightforward preparation from
12
13 commercial starting materials is described in the Supporting Information.
14
15

16
17 All was ready for preparation of the three dual conjugates **1-3**, where the main modules could be
18
19 connected through common synthesis pathways. Thus, as shown in Scheme 3, parallel BOP-
20
21 promoted condensation of carboxylic acid **13** with either amines **14**, **16** or **18** provided access to
22
23 the respective alkyne-terminating amides **15**, **17**, or **19** in good isolated yields (64-88%). Copper-
24
25 catalyzed 1,3-dipolar cycloaddition between these alkynes and the previous c(AmpRGD) azide **7**
26
27 (two-fold equivalents in case of the dimeric execution in eq. 3) followed by acidic deprotection
28
29 gave conjugates **1-3** in good yields and purity after semipreparative reverse-phase HPLC
30
31
32
33
34 purification (43-70% yields; 96-98% purity, recovered as TFA salts).
35
36
37
38
39
40
41
42
43
44
45
46
47
48
49
50
51
52
53
54
55
56
57
58
59
60

Scheme 3. Modular Synthesis of the Sunitinib-c(AmpRGD) Conjugates 1-3^a

^aReagents and conditions: (a) BOP, DIPEA, DCM/DMF (2:3), rt; (b) (i) azide **7**, Cu(OAc)₂, Na L-asc, H₂O/DMF, rt; (ii) TFA/TIS/H₂O (95:2.5:2.5), rt.

In Vitro Stability of Conjugates 1-3. The in vitro stability of conjugates **1-3** in 80% v/v rat and human plasma was firstly evaluated by HPLC-UV-Vis analysis. The cyclopeptides were incubated and analyzed up to 8 h, as detailed in Table 1 (see also the Supporting Information). Invariably and regardless their intimate structure, compounds **1-3** showed complete resistance to rat and human plasma degradation during the observed time. This demonstrated that the covalent connection of the modules resulted in robust conjugates anticipating that, whatever the biological response, it would be the result of the interaction of the cell environment with the integral, preserved structure of the conjugates and not the individual detached components. Whether this would translate into a benefit or disadvantage in biological assays remained to be seen.

Table 1. In Vitro Plasma Stability of Compounds 1-3 vs Sunitinib

Compound	Rat plasma (% compd at 8h) ^a	Human plasma (% compd at 8h) ^a
sunitinib	97.3 (±9.1)	102.3 (±5.2)
1	88.2 (±12.7)	99.0 (±10.9)
2	104.1 (±3.3)	106.6 (±11.5)
3	108.8 (±10.5)	98.6 (±15.4)

^aPercentage of compound remaining after 8 h of incubation in 80% v/v plasma, 37 °C, protected from light. Reported are Means ± SD.

Lipophilicity and Cellular Uptake of Conjugates 1-3. At physiological pH, compounds **1-3** proved highly hydrophilic in accordance with the measured negative values of the $\text{Log}D_{\text{Oct},7.4}$ (i.e. the distribution coefficient in *n*-octanol/buffer at pH 7.4, Table 2). As expected, attachment of the c(AmpRGD) module to the sunitinib-like portion turned the lipophilic character of the drug to hydrophilic, which was magnified by the pegylated linker (compounds **2** and **3** vs **1**) and the dipeptide presentation (**3** vs **1** and **2**).

Table 2. Lipophilicity and Cellular Uptake of Compounds 1-3 and Sunitinib in EPCs

Compound	Log $D_{\text{oct},7.4}^a$	MW	Intracellular Content (nmol/mg prot) (1 h) ^b	Cell uptake (pmol/min /mg prot) (1 h)	Log Cell Uptake (1 h)	Intracellular Content (nmol/mg prot) (8 h) ^b
sunitinib	2.51	398.5	5.72 (± 0.71)	95.3	1.98	2.90 (± 0.40)
1	- 2.03	960.0	0.26 (± 0.02)	4.3	0.64	0.22 (± 0.02)
2	- 2.56	1078.2	0.48 (± 0.07)	8.0	0.90	0.43 (± 0.09)
3	- 3.02	1788.9	0.94 (± 0.02)	15.7	1.19	0.54 (± 0.03)

^aDistribution coefficient in the n-octanol/buffer system, pH 7.4. Reported are Means \pm SD.
^bEPCs were incubated with 1 μ M final concentration of test compound. After 1 h, the medium containing the tested compounds was removed and intracellular content was quantified immediately and after 8 h. Experiments were conducted in triplicate and data were expressed as nmol/mg of total cell proteins in each sample.

The capability of endothelial progenitor cells (EPCs) to internalize conjugates **1-3** as compared to free sunitinib was next investigated. Total intracellular concentrations of **1-3** and sunitinib were measured by HPLC-ESI-MS/MS. EPCs were incubated in standard conditions for 1 h in the presence of the different compounds at 1 μ M final concentration (see also Experimental and Figure S1 in the Supporting Information). As illustrated in Table 2, all compounds were detected in the intracellular extracts, with the small-sized sunitinib drug showing maximum levels at 1 h, while conjugates **1-3** were found in the cell extract to a much lesser extent. In particular, compound **1** showed a scarce entrance in cells after 1 h treatment, which remained almost

1
2
3 invariable after 8 h. Pegylated counterpart **2**, having similar molecular weight, almost doubled its
4
5 ability to enter cells as compared to **1** at both 1 h and 8 h treatment. Finally, dimeric RGD
6
7 conjugate **3**, notwithstanding its higher molecular weight, showed a 4-fold and 2-fold ability to
8
9 enter cells as compared to **1** and **2**, respectively.
10
11

12
13 These data are quite interesting since they emphasize the following points: *i*) the requisite
14
15 delivery of the sunitinib-like moiety inside cells is provided by conjugates **1-3**, even if the
16
17 internalization is not as efficient as the free drug, and *ii*) the amount of each conjugate (expressed
18
19 as pmol/min/mg prot) which passes through the EPC membrane in the first hour is, on a log
20
21 scale, inversely related to its lipophilicity, expressed by the distribution coefficient at pH 7.4, *i.e.*
22
23 $\text{Log}(\text{cell uptake}) = -0.55(\pm 0.04)\text{log } D_{\text{oct}, 7.4} - 0.50(\pm 0.10)$; $n=3$; $r^2 = 0.995$; $s=0.03$; $F=191$. The
24
25 more hydrophilic and bulkier **3** is more efficiently internalized than **1**; the dependence of the
26
27 internalized content upon the RGD presentation (monomeric vs dimeric) suggests a direct
28
29 involvement of the RGD moiety during the internalization process possibly via $\alpha_V\beta_3$ -mediated
30
31 endocytosis.⁵²⁻⁵⁷ The assay was repeated for compounds **2** and **3** in the presence of excess $\alpha_V\beta_3$
32
33 integrin ligand **8** (100 μM). Significant decrease of cell uptake was witnessed for both
34
35 compounds (Table S1 in the Supporting Information) further corroborating the notion of an
36
37 active role of this integrin during internalization.
38
39
40
41
42
43
44
45

46 **Solid-phase receptor binding assay.** The integrin activity and selectivity profile of compounds
47
48 **1-3** were firstly evaluated by measuring their ability to bind to human, isolated $\alpha_V\beta_3$ and $\alpha_5\beta_1$
49
50 integrin receptors by competitive displacement assays using either biotinylated vitronectin VN
51
52 (for $\alpha_V\beta_3$) or biotinylated fibronectin FN (for $\alpha_5\beta_1$). To better evaluate the impact of the sunitinib
53
54 moiety on binding capability, the results were compared to those obtained for the unconjugated
55
56
57
58
59
60

counterpart c(AmpRGD)-(CH₂)₂NH₂ and commercial ligand c(RGDfV). As shown in Table 3, compounds **1-3** exhibited one-digit nanomolar affinity toward $\alpha_v\beta_3$ integrin, which was even superior to the unconjugated AmpRGD-based counterpart and showed in all cases an appreciable $\alpha_v\beta_3/\alpha_5\beta_1$ selectivity. Compound **3**, bearing a 2-fold RGD repeat, showed an increased binding affinity as compared to monomer **2**, even if it was lower than **1**. Overall, the presence of a sunitinib-linker cargo attached to the integrin-recognizing RGD unit did not compromise the exquisite binding affinity and selectivity of these conjugates.

Table 3. Inhibition of Biotinylated VN and FN Binding to $\alpha_v\beta_3$ and $\alpha_5\beta_1$ Receptors, Respectively^a

Compound	IC ₅₀ (nM)±SD for $\alpha_v\beta_3$	IC ₅₀ (nM)±SD for $\alpha_5\beta_1$
1	1.24±0.01	30.7±17.7
2	5.1±0.6	101.3±31.3
3	3.8±0.6	95.8±46.7
c(AmpRGD)-(CH ₂) ₂ NH ₂	6.1±1.6 ^b	151.6±67.6 ^b
c(RGDfV)	3.2±1.3 ^b	166.0±28.0 ^c

^aIC₅₀ values were calculated as the concentration of compound required for 50% inhibition of biotinylated VN or FN binding to human, isolated receptors. Each data point represents the average of triplicate wells; data analysis was carried out by nonlinear regression analysis using GraphPad Prism software. Each experiment was repeated in duplicate. ^bRef. 42. ^cRef. 43.

Inhibition of EPC adhesion to the $\alpha_v\beta_3$ -ligand vitronectin using conjugates 1-3. The synthesized compounds **1-3** were evaluated for their ability to inhibit the adhesion of natural ligand VN to $\alpha_v\beta_3$ -overexpressing cells. Endothelial progenitor cells were chosen due to their abundant $\alpha_v\beta_3$ integrin receptor expression (as certified by flow cytometric analysis, Figure S2) and for their recognized role in tumor angiogenesis.⁵⁹⁻⁶¹ The assay of adhesion inhibition was

performed in the presence of 2.0 mmol/L MnCl_2 to switch $\alpha_v\beta_3$ integrin to its activated form with increasing concentrations of compounds **1**, **2** and **3** (1, 10, 100, 1000, 10000 nM); for comparison purposes, sunitinib alone, unconjugated c(AmpRGD) **8**, and a combination of both were also assayed.

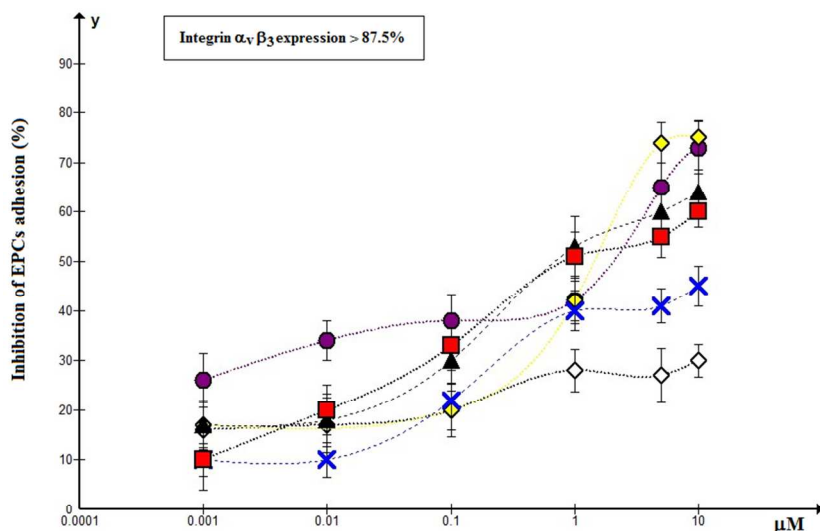


Figure 4. Inhibition of EPCs adhesion to VN in the presence of compounds **1-3**, **8**, sunitinib, and the combination sunitinib+**8** (▲ compound **1**; × compound **2**; ■ compound **3**; ● compound **8**; ◇ sunitinib; ◆ compound **8**+sunitinib). Top insert indicates the percentage of $\alpha_v\beta_3$ integrin expression in EPCs. The inhibitory activity was calculated as percentage of cell adhesion to VN in untreated cells and was expressed as mean±SD. Experiments were carried out in triplicate.

As shown in Figure 4, conjugated cyclopeptides **1** and **3** strongly inhibited cell adhesion in a dose-related manner with IC_{50} values nearly approaching 500 nM, while conjugate **2** showed a

1
2
3 less efficient activity (IC_{50} ca 10 μ M); notably, the binding capability of compounds **1** and **3** was
4
5 even better than the unconjugated counterpart **8** (IC_{50} 1.8 μ M). As expected, the binding
6
7 capability of sunitinib alone remained negligible at these concentrations. Overall, the covalent
8
9 conjugation of the c(AmpRGD) portion to the sunitinib-like moiety as described in the diverse
10
11 topologies of compounds **1-3** does not significantly alter the ligand binding capability towards
12
13 these endothelial $\alpha_v\beta_3$ -overexpressing cells.
14
15
16
17

18
19 **Effect of conjugates 1-3 on cell proliferation and cell viability.** The effect of the different
20
21 compounds was evaluated on EPCs in a proliferation assay performed in the presence of VEGF-
22
23 A (20 ng/mL), and the various compounds **1-3**, **8**, sunitinib, and **8**+sunitinib at 1 μ M
24
25 concentration every 24 h. The effect was followed after 24 h, 48 h and 72 h exposure. Cell
26
27 proliferation was measured by cell count and cell viability was evaluated using trypan blue
28
29 exclusion assay (Figure 5). After the first 24 h treatment, conjugates **1-3** showed inhibition of
30
31 VEGF-induced proliferation of 46%, 24%, and 41%, respectively, with respect to untreated cells.
32
33 On the other hand, sunitinib inhibited cell proliferation of 33%, and the combination of sunitinib
34
35 with compound **8** poorly impacted cell proliferation. After 48 h treatment, conjugates **1-3** and
36
37 sunitinib alone maintained almost the same level of inhibition of proliferation. Interestingly, the
38
39 combination of sunitinib and compound **8** revealed a 23% of inhibition. After 72 h, inhibition of
40
41 EPCs proliferation found in cells treated with compound **3** was similar to that of cells exposed to
42
43 sunitinib, while other treatments did not show a significant inhibition of proliferation.
44
45
46
47
48

49
50 During the entire experiment, cell viability was monitored and no significant difference was
51
52 found in EPCs exposed either to the conjugated compounds or to separate drugs.
53
54
55
56
57
58
59
60

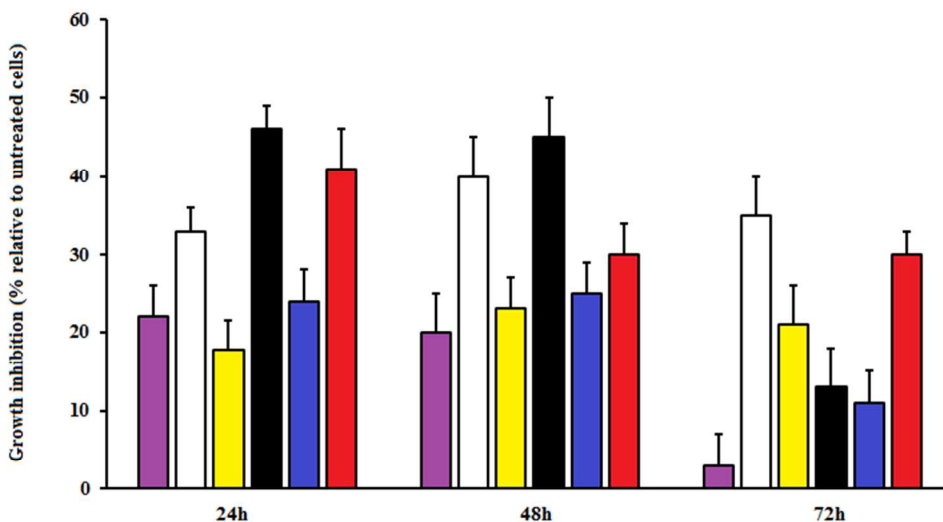


Figure 5. Effect of the different compounds on VEGF-mediated EPCs proliferation. EPCs were grown in a serum and growth factor-free medium containing 20 ng/mL VEGF-A. Cells were exposed to 1 μ M concentration of different compounds every 24 h (■ compound 8, □ sunitinib; ■ compound 8+sunitinib, ■ compound 1, ■ compound 2, ■ compound 3). After 24 h, 48 h, and 72 h incubation, cells were counted and cell viability was assessed. Representative of three independent experiments.

Inhibition of TKI activity by conjugates 1-3. To evaluate whether conjugation within 1-3 would affect the TKI activity of the sunitinib-like portion toward its targeted kinases, we firstly evaluated the inhibitory activity of representative compound 3 against human recombinant PDGFR β and VEGFR2. As shown in Table 4, IC₅₀ values were in the nanomolar range, slightly superior than those reported for sunitinib,¹³ demonstrating that appendage of the two RGD moieties and linker was not detrimental for TKI activity in vitro.

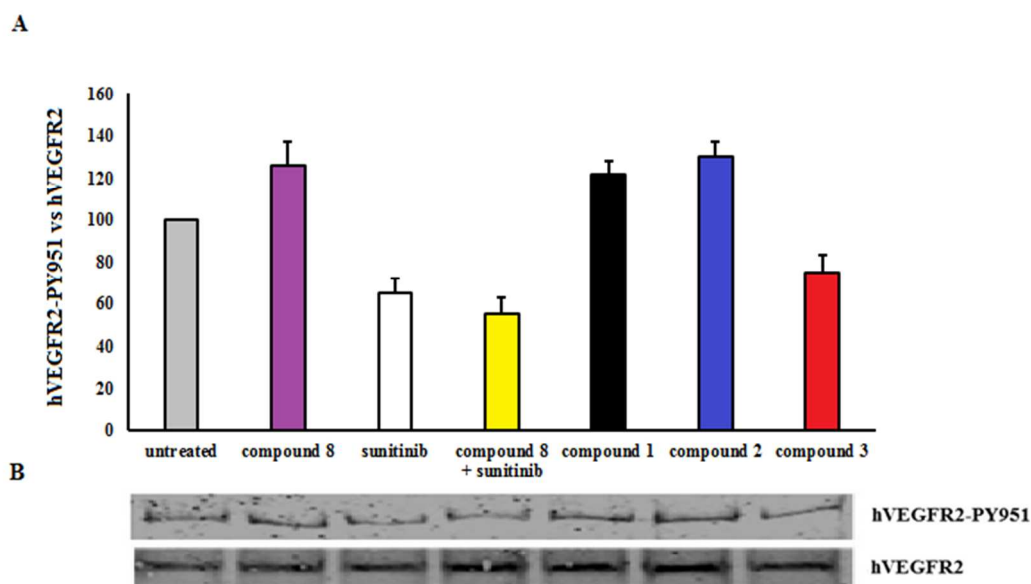
Table 4. Inhibition of TKI Activity for Compound 3 and the Reference Compound**Sunitinib against Human Recombinant PDGFR β and VEGFR2^a**

Compound	PDGFR β (nM)	VEGFR2 (nM)
3	9	420
sunitinib	2 ^b	80 ^b

^aIC₅₀ values for **3** were calculated as the concentration of compound required for 50% inhibition of control specific activity (staurosporine). Each data point represents the average of duplicate wells; data analysis was carried out by nonlinear regression analysis using software developed at Cerep (Hill software). ^bRef. 13.

The ability of compounds **1-3** to inhibit VEGF-stimulated VEGFR2 phosphorylation was investigated by Western blotting using EPCs, which were proven to express high levels of VEGFR2 (besides $\alpha_v\beta_3$). Sunitinib alone, c(AmpRGD) **8** alone, and a combination of the two were also assayed for comparison purposes. Percent inhibition at 1 μ M concentration is reported in the densitometric analysis histogram (Figure 6). EPCs were treated for 1 h with the different compounds and then activated with 50 ng/mL VEGF-A for 5min⁶² before cell lysis for VEGFR2 phosphorylation detection. Among the different compounds, **1**, **2** and **8** showed a weak induction of VEGFR2 phosphorylation that might be the result of the synergistic intracellular interaction between $\alpha_v\beta_3$ and VEGFR2 probably through Src domains leading to a mild activation of the VEGF receptor.^{32,35} As mentioned before, the biological behavior of monomeric compounds **1** and **2** might be influenced more by their RGD moiety rather than the sunitinib moiety, as a consequence of their weak propensity to enter EP cells. Interestingly, dimeric compound **3** induced a marked reduction of VEGFR2 phosphorylation, comparable to that found in EP cells

1
2
3 exposed to sunitinib alone or to the combination of sunitinib + **8**; and this would support the
4
5 notion that the biological behavior of compound **3** is heavily influenced by its sunitinib moiety,
6
7 likely due to the enhanced ability to be delivered to the intracellular compartment through the
8
9 double RGD moieties. Overall, the TKI activity of compound **3** is attributable to the direct
10
11 interaction with the Y951 domain of VEGFR2 (as sunitinib does) supporting the evidence that **3**
12
13 acts as genuine VEGFR2 antagonist.
14
15
16



33
34
35
36
37
38
39
40
41
42
43
44
45
46
47
48
49
50
51
52
53
54
55
56
57
58
59
60

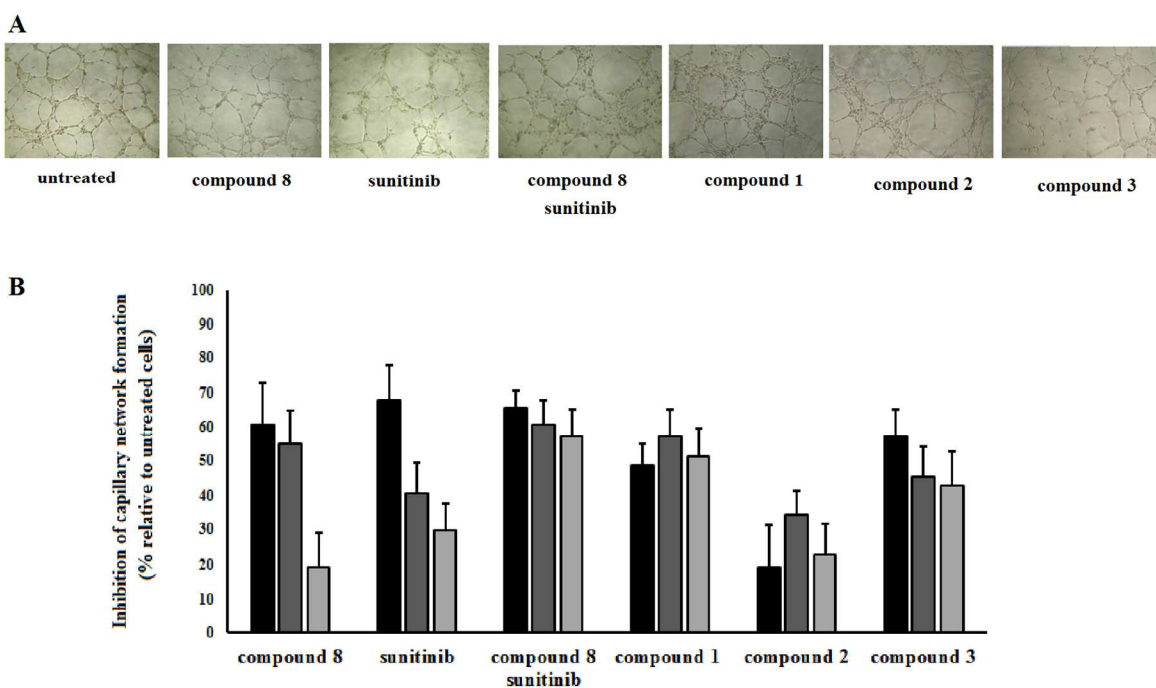
Figure 6. Inhibition of VEGFR2 phosphorylation in EPCs treated for 1 h with 1 μ M concentration of different compounds followed by VEGF-A activation (50 ng/mL) for 5 min. A) densitometric analysis of the inhibition of VEGF-induced VEGFR2 phosphorylation; B) western blot analysis. Results are reported as the mean \pm SD of percent of inhibition of VEGFR phosphorylation compared to VEGF-treated cells. Representative of three independent experiments.

1
2
3 **Conjugates 1-3 inhibit the angiogenic process in vitro and in vivo.** The ability of conjugates
4 **1-3** to interfere with EP cells in organizing capillary network in vitro was determined. Cells were
5
6 seeded on Matrigel and exposed to a medium containing VEGF-A (20 ng/mL). Cells were
7
8 incubated for 6 h in the presence of conjugates **1-3**, unconjugated c(AmpRGD) **8**, sunitinib, and
9
10 the combination **8**+sunitinib at 0.01, 0.1, and 1.0 μ M concentrations. As shown in Figure 7A, a
11
12 significant or even dramatic reduction in the number of newly formed tubules was observed
13
14 when EP cells were incubated on Matrigel with the various compounds. The quantification was
15
16 performed by measuring the number of loops formed by connecting capillary projections
17
18 (branches) and expressed as percentage of reduction compared to untreated cells, as reported in
19
20 Figure 7B.
21
22
23
24
25
26
27

28 Unconjugated c(AmpRGD) **8** shows a good and dose-related anti-angiogenic activity which is
29
30 likely due to the inhibitory interaction between the RGD moiety and the extracellular binding
31
32 domain of $\alpha_v\beta_3$ integrin. Slightly superior anti-angiogenic response is witnessed with sunitinib
33
34 alone, which clearly owes this behavior to its interaction with the intracellular domain of
35
36 different kinases, including VEGFR2. Treating EPCs with the combination **8**+sunitinib results in
37
38 a remarkable dose-dependent (slightly sloped) anti-angiogenic trend, with an exceptional 60%
39
40 inhibition at 10 nM, much higher than that observed in **8** (19%) and sunitinib (30%) separately.
41
42 Passing to conjugates **1-3**, the inhibitory activity of angiogenesis is more pronounced for **1** and **3**
43
44 than for **2**. In particular, for monomeric compound **1** and dimeric derivative **3**, the anti-
45
46 angiogenesis activity is similar to that of the single **8** or sunitinib at both 1 μ M and 0.1 μ M
47
48 concentrations, while it is highly improved (52% for **1** and 43% for **3**) at 10 nM, somehow
49
50 paralleling the behavior of the combination. This demonstrates that for both the combined and
51
52 conjugated ingredients, a favorable synergy could exist, given by both the extracellular RGD-
53
54
55
56
57
58
59
60

1
2
3 integrin interaction (likely provided by the non-internalized fraction of compounds) and the
4
5 sunitinib-VEGFR2 kinase interaction (provided by the amount of internalized compound, see
6
7 also uptake data). Indeed, the partial internalization of the conjugates may be considered a
8
9 benefit allowing the contemporary action both outside and inside cells.
10
11

12
13
14 Overall, the association of the two active modules either in the guise of a combination or as a
15
16 covalent conjugate is beneficial to gain anti-angiogenic effect in vitro. Which of the two options
17
18 is better has to be judged after in vivo anti-angiogenesis evaluation, which is able to measure the
19
20 putative targeting effect within the covalent conjugates.
21
22
23

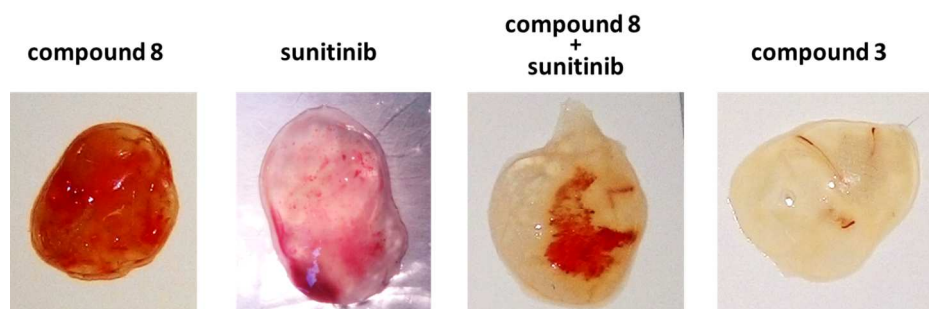


51 **Figure 7.** In vitro inhibition of tubulogenesis in VEGF-A activated (20 ng/mL) EPCs seeded on
52
53 Matrigel and incubated for 6 h with compounds 1-3, c(AmpRGD) 8, sunitinib, and 8+sunitinib at
54
55 1 μM (black), 0.1 μM (dark grey), and 0.01 μM (grey) concentrations. A) Representative images
56
57
58
59
60

1
2
3 of the different treatments at 1 μ M concentration. B) Histograms refer to the inhibition of
4
5 branches development as compared to untreated cells and expressed as percentage.
6
7

8 Representative of three independent experiments.
9
10

11
12
13
14
15 We next measured the ability of conjugate **3** (as compared to **8**, sunitinib and their combination)
16
17 to block angiogenesis in vivo using a Matrigel plug assay. We chose compound **3** for this study
18
19 as it had the strongest binding to EPCs, it was best internalized, it was the most effective in
20
21 inhibiting VEGFR2 phosphorylation and capillary tube formation. Despite the very preliminary
22
23 character of the data obtained, we found that in vivo angiogenesis is scarcely impaired by
24
25 unconjugated compound **8**, while it is downregulated by sunitinib treatment (Figure 8). This
26
27 inhibition was comparable to that obtained in the co-treatment, while the injection of compound
28
29 **3** revealed a consistent reduction of in vivo angiogenesis. These results corroborate the
30
31 substantial role of conjugate **3** as an anti-angiogenic tool in vivo and substantiate the hypothesis
32
33 according to which the covalent conjugation of two key angiogenesis-related players (as in **3**)
34
35 results in a synergic action, even superior to their simple combination.
36
37
38
39
40
41



53
54 **Figure 8.** Inhibition of in vivo angiogenesis in Matrigel plugs implanted in FVB mice. Matrigel
55
56 plugs contained VEGF-A/heparin+10 mg/kg sunitinib or equivalent quantity within **8** or **3**
57
58
59
60

1
2
3 (compound **8**, sunitinib, sunitinib+**8**, compound **3**). Plugs were removed from mice and
4
5
6 photographed after 4 days.
7
8
9

10 11 12 CONCLUSIONS

13
14
15 Three novel molecules, compounds **1-3**, were efficiently synthesized and characterized, which
16
17 featured the robust covalent linkage of a sunitinib-like portion to one or two cyclic aminoproline
18
19 RGD moieties. Subsequent biological investigations gave important clues about the relative
20
21 weight of the active modules within the conjugates. Overall, compound **3** seems to best
22
23 summarize the structural characteristics required for optimal biological response, where both the
24
25 RGD and the sunitinib modules may exert an active role. The preliminary, relevant anti-
26
27 angiogenic effect of compound **3** in mice assesses its potential as an effective tool against tumor-
28
29 associated angiogenesis and is even superior than the simple combination of the two discrete
30
31 modules. This work stands as a proof-of-concept of how anti-angiogenic small molecules may be
32
33 selectively delivered to cells through simple, super-targeted anti-angiogenic conjugated
34
35 molecules to be used in tumor-related or angiogenesis-related therapy.
36
37
38
39
40
41
42
43
44
45

46 47 EXPERIMENTAL SECTION

48
49 **Chemistry. General.** All chemicals were of the highest commercially available quality and were
50
51 used without further purification. Solvents were dried by standard procedures and reactions
52
53 requiring anhydrous conditions were performed under nitrogen or argon atmosphere. H-Gly-2-
54
55 CITrt resin (loading 0.63 mmol/g) was purchased from Novabiochem, (2*S*,4*S*)-Fmoc-4-amino-1-
56
57
58
59
60

1
2
3 Boc-pyrrolidine-2-carboxylic acid (**4**) from PolyPeptide and all other reagents from Alfa Aesar,
4 TCI, or Sigma-Aldrich. Flash column chromatography was performed using 40-63 μm silica gel
5
6 using the indicated solvent mixtures. Automated flash column chromatography was carried out
7
8 with the Biotage Isolera One system using Biotage KP-Sil cartridges (direct phase) or KP-C18-
9
10 HS (reverse phase). Melting points (mp) were measured with an optical Optiphot2-Pol thermo-
11
12 microscope and are uncorrected. Optical rotations were measured using a Perkin-Elmer model
13
14 341 polarimeter at ambient temperature using a 100 mm cell with a 1 mL capacity and are given
15
16 in units of $10^{-1} \text{ deg cm}^2 \text{ g}^{-1}$. ESI-mass spectra were recorded on API 150EX apparatus and are
17
18 reported in the form of (m/z). HPLC purifications were performed on a Prostar 210 apparatus
19
20 (Varian, UV detection) equipped with C₁₈-10 μm columns (Discovery BIO Wide Pore 10 \times 250
21
22 mm or 21.2 \times 250 mm). Routine NMR spectra were recorded on Avance 300 or 400 (Bruker)
23
24 NMR spectrometers. Chemical shifts (δ) are reported in parts per million (ppm) with TMS
25
26 (CDCl_3), CD_2HOD , and HOD resonance peaks set at 0, 3.31, and 4.80 ppm, respectively.
27
28 Multiplicities are indicated as s (singlet), d (doublet), t (triplet), q (quartet), m (multiplet), and b
29
30 (broad). Coupling constants, J , are reported in Hertz. ^1H and ^{13}C NMR assignments are
31
32 corroborated by 1D and 2D experiments (gCOSY and gHSQC sequences). High resolution mass
33
34 analysis (ESI) was performed on LTQ ORBITRAP XL Thermo apparatus. Purity of all tested
35
36 compounds was determined by analytical high-pressure liquid chromatography (HPLC) and was
37
38 in the 96 - >99% range.
39
40
41
42
43
44
45
46
47

48
49 *Materials.* H-Gly-2-ClTrt resin (loading 0.63 mmol/g), (2*S*,4*S*)-Fmoc-4-amino-1-Boc-
50
51 pyrrolidine-2-carboxylic acid (**4**), Fmoc-Asp(*t*Bu)-OH; Fmoc-Arg(Pmc)-OH, 2,4,6-collidine,
52
53 piperidine, glacial acetic acid, 4-pentynoic acid, 5-fluoroisatin, ethyl 5-formyl-2,4-
54
55 dimethylpyrrole-3-carboxylate, triethylene glycol, *N*-Boc-ethylenediamine, propargyl bromide,
56
57
58
59
60

1
2
3 acetaldehyde, 2-[2-(2-aminoethoxy)ethoxy]ethanol, 3,5-dihydroxybenzoic acid were
4
5 commercially available and were used as such without further purification. Sunitinib malate salt
6
7 was purchased by LC Laboratories (USA) with a purity of >99%.
8
9

10
11 *Synthesis of the c(AmpRGD) Azide 7.* To a solution of linear tetrapeptide **6** (137 mg, 0.16
12
13 mmol, 1 equiv) in dry DCM (35 mL), 2,4,6-collidine (52 μ L, 0.39 mmol, 2.5 equiv) was
14
15 added. The mixture was stirred under argon at room temperature, and added dropwise to a
16
17 solution of HATU (119 mg, 0.31 mmol, 2 equiv) and HOAt (43 mg, 0.31 mmol, 2 equiv) in
18
19 dry DMF (5mL) and dry DCM (30 mL). The reaction mixture was degassed by argon/vacuum
20
21 cycles (3 \times) and left to stir under argon at room temperature for 5 h. After completion, the
22
23 solution was concentrated under vacuum, treated with aq NaHCO₃ saturated solution and
24
25 extracted with EtOAc (4 \times). The combined organic layers were dried with MgSO₄, filtered
26
27 and evaporated under reduced pressure, keeping the temperature under 50 °C. The crude was
28
29 purified by reverse phase flash chromatography [H₂O (0.1% TFA)/MeCN: linear gradient
30
31 80:20 to 20:80] furnishing the protected c(AmpRGD)-N₃ **7** (90 mg, yield 67%) as a white
32
33 solid; mp 118.6 °C; $[\alpha]_D^{25} = +19.2$ (c 0.5; MeOH). ¹H NMR (400 MHz, MeOD) δ 4.64 (dd, J
34
35 = 6.3, 5.6 Hz, 1H, H α Asp), 4.44 (ddd, J = 6.9, 6.9, 2.0 Hz, 1H, H4), 4.16 (d, J = 13.9 Hz, 1H,
36
37 H α Gly), 4.08 (t, J = 7.5 Hz, 1H, H α Arg), 3.64 (d, J = 9.2 Hz, 1H, H2), 3.34 (d, J = 13.9 Hz,
38
39 1H, H α Gly), 3.30 (t, J = 6.6 Hz, 2H, H δ Arg), 3.27-3.13 (m, 3H, H1'a,b + H5a), 3.04 (bd, J =
40
41 9.6 Hz, 1H, H5b), 2.76-2.63 (m, 6H, H β Asp + CH₂ Pmc + H4'a,b), 2.59 (s, 3H, CH₃ Pmc),
42
43 2.57 (s, 3H, CH₃ Pmc), 2.41 (ddd, J = 13.6, 9.5, 7.1 Hz, 1H, H3a), 2.12 (s, 3H, CH₃ Pmc),
44
45 1.99 (d, J = 13.6 Hz, 1H, H3b), 1.86 (t, 2H, CH₂ Pmc), 1.74-1.69 (m, 2H, H β Arg), 1.65-1.62
46
47 (m, 6H, H γ Arg + H2' + H3'), 1.46 (s, 9H, *t*Bu), 1.33 (s, 6H, CH₃ Pmc). ¹³C NMR (75 MHz,
48
49 MeOD) δ 177.3 (Cq), 175.4 (Cq), 170.6 (Cq), 170.1 (Cq), 169.8 (Cq), 156.8 (Cq), 153.5 (Cq),
50
51
52
53
54
55
56
57
58
59
60

1
2
3 138.5 (Cq), 135.3 (Cq), 134.9 (Cq), 133.5 (Cq), 123.8 (Cq), 118.2 (Cq), 81.0 (Cq), 73.7
4
5 (CH₂), 62.7 (CH₂), 60.0 (CH₂), 55.1 (CH), 52.3 (CH₂), 51.0 (CH₂), 49.8 (CH), 49.1 (CH),
6
7 44.4 (CH₂), 40.1 (CH), 37.3 (CH₂), 36.1 (CH₂), 32.6 (CH₂), 27.1 (3C, CH₃), 26.9 (CH₂), 26.5
8
9 (CH₂), 25.8 (2C, CH₃), 25.7 (CH₂), 21.2 (CH₂), 17.8 (CH₃), 16.7 (CH₃), 11.1 (CH₃). HRMS
10
11 (ES⁺) C₃₉H₆₁N₁₁O₉S calcd for [M+H]⁺ 860.4447, found 860.4470.
12
13

14
15 *Synthesis of the c(AmpRGD) Amine 8.* The cyclic tetrapeptide **7** (29 mg, 0.03 mmol) was
16
17 dissolved in EtOH (4 mL) and a catalytic amount of 10% palladium on carbon was added. The
18
19 reaction vessel was degassed under vacuum and thoroughly purged with hydrogen (3 ×). The
20
21 resulting heterogeneous mixture was stirred overnight under hydrogen at room temperature, then
22
23 the catalyst was filtered off and the filtrate was concentrated under vacuum. The protected
24
25 intermediate AmpRGD-NH₂ (27 mg, 0.03 mmol) was dissolved in 1.6 mL of a TFA/TIS/H₂O
26
27 (95:2.5:2.5) mixture and stirred at room temperature for 2.5 h. Then, the solvent was evaporated
28
29 and the crude residue was thoroughly washed with Et₂O (4 ×) and petroleum ether (2 ×).
30
31
32 Preparative RP-HPLC purification was performed [C₁₈-10 μm column, 21.2 × 250 mm; solvent
33
34 A: H₂O (0.1% TFA) and solvent B: MeCN, flow rate 8 mL/min; detection 220 nm] using a linear
35
36 gradient from 100% A to 25% B in 25 min. The removal of the solvent under vacuum, keeping
37
38 the temperature under 50 °C, furnished c(AmpRGD)-NH₂ **8** (18.4 mg, TFA salt, yield 91%) as a
39
40 colourless glassy solid; [α]_D²⁵ = -13.3 (c 1.0, H₂O). ¹H NMR (400 MHz, D₂O) δ 4.60 (dd, *J* =
41
42 6.2, 6.2 Hz, 1H, H_α Asp), 4.52 (d, *J* = 10.8 Hz, 1H, H₂), 4.26 (bt, *J* = 4.9 Hz, 1H, H₄), 4.12 (dd,
43
44 *J* = 7.5, 7.5 Hz, 1H, H_α Arg), 3.94 (d, *J* = 13.9 Hz, 1H, H_α Gly), 3.93 (m, 1H, H_{5a}), 3.37 (bd, *J*
45
46 = 8.8 Hz, 1H, H_{5b}), 3.21 (m, 2H, H_{4'}), 3.09 (t, *J* = 6.8 Hz, 2H, H_δ Arg), 2.90–2.81 (m, 3H, H_{1'}
47
48 + H_{3a}), 2.80 (d, *J* = 5.9 Hz, 2H, H_β Asp), 2.42 (bd, *J* = 15.2 Hz, 1H, H_{3b}), 1.68–1.46 (m, 8H,
49
50 H_β Arg + H_γ Arg + H_{2'} + H_{3'}). ¹³C NMR (100 MHz, D₂O) δ 176.2 (Cq), 174.5 (Cq), 172.7 (Cq),
51
52
53
54
55
56
57
58
59
60

1
2
3 171.2 (2C, Cq), 156.9 (Cq), 66.0 (CH), 60.2 (CH₂), 56.1 (CH), 49.9 (CH), 44.6 (CH₂), 40.6
4
5 (CH₂), 38.8 (CH₂), 35.1 (CH₂), 35.0 (CH₂), 34.9 (CH₂), 26.5 (CH₂), 24.6 (CH₂), 23.8 (CH₂), 22.3
6
7 (CH₂). HRMS (ES⁺) C₂₁H₃₇N₉O₆ calcd for [M+H]⁺ 512.2940, found 512.2932.

8
9
10
11 *Synthesis of compound 15.* To a solution of **13** (94 mg, 0.31 mmol, 1 equiv) in dry DCM (1.5
12 mL) and dry DMF (2.5 mL), BOP (70 mg, 0.16 mmol, 1.3 equiv) and DIPEA (85 μL, 0.49
13 mmol, 4 equiv) were added and, after 5 min, a solution of **14** (103 mg, 0.41 mmol, 1.3 equiv) in
14 dry DCM (1.5 mL) and dry DMF (1 mL) was added. The reaction was stirred under argon at
15 room temperature, protected from light. A yellow precipitate started to form after 1 h. After 5 h
16 the reaction was over and Et₂O (3 mL) and petroleum ether (3 mL) were added to the mixture.
17 The solid was collected by vacuum filtration and washed with H₂O (3 ×) furnishing compound
18 **15** (116 mg, yield 88%) as an orange solid; mp > 220 °C. ¹H NMR (400 MHz, DMSO-d₆) δ 13.69
19 (s, 1H, NH), 10.89 (s, 1H, NH), 8.02 (bt, *J* = 4.5 Hz, 1H, NH), 7.76 (dd, *J* = 9.5, 2.0 Hz, 1H,
20 H4), 7.72 (s, 1H, H1'), 7.60 (bt, *J* = 5.0 Hz, 1H, NH), 6.92 (ddd, *J* = 8.8, 8.8, 2.0 Hz, 1H, H6),
21 6.85 (dd, *J* = 9.2, 4.4 Hz, 1H, H7), 3.28 (m, 2H, CH₂), 3.24 (m, 2H, CH₂), 2.76 (t, *J* = 2.4 Hz,
22 ≡CH), 2.44 (s, 3H, CH₃), 2.42 (s, 3H, CH₃), 2.37 (m, 2H, CH₂), 2.29 (t, *J* = 7.1 Hz, 2H, CH₂).
23 ¹³C NMR (100 MHz, DMSO-d₆) δ 171.1 (Cq), 170.0 (Cq), 165.4 (Cq), 158.6 (d, ¹*J*_{CF} = 233 Hz,
24 Cq), 137.1 (Cq), 135.0 (Cq), 130.8 (Cq), 127.6 (d, ³*J*_{CF} = 10 Hz, Cq), 126.3 (CH), 125.3 (Cq),
25 121.0 (Cq), 115.1 (Cq), 112.8 (d, ²*J*_{CF} = 25 Hz, CH), 110.4 (d, ³*J*_{CF} = 8 Hz, CH), 106.3 (d, ²*J*_{CF} =
26 26 Hz, CH), 84.2 (Cq), 71.7 (CH), 46.6 (CH₂), 34.8 (CH₂), 19.3 (CH₂), 14.7 (CH₂), 13.8 (CH₃),
27 11.0 (CH₃). HRMS (ES⁺) C₂₃H₂₃FN₄O₃ calcd for [M+H]⁺ 423,1827, found 423,1823.

28
29
30
31
32
33
34
35
36
37
38
39
40
41
42
43
44
45
46
47
48
49
50
51
52 *Synthesis of compound 17.* To a stirred suspension of **13** (11 mg, 0.04 mmol, 1 equiv) in dry
53 DMF (500 μL), BOP (21 mg, 0.05 mmol, 1.3 equiv) and DIPEA (26 μL, 0.15 mmol, 4 equiv)
54 were added and, after 5 min, a solution of **16** (15 mg, 0.04 mmol, 1.1 equiv) in dry DCM (400
55
56
57
58
59
60

1
2
3
4
5
6
7
8
9
10
11
12
13
14
15
16
17
18
19
20
21
22
23
24
25
26
27
28
29
30
31
32
33
34
35
36
37
38
39
40
41
42
43
44
45
46
47
48
49
50
51
52
53
54
55
56
57
58
59
60

μL) was added. The reaction mixture was stirred under argon at room temperature for 3 h protected from light. After reaction completion, the solvent was evaporated under reduced pressure, the residue was washed with water ($3 \times$), and the solvent was removed by a Pasteur pipette. The yellow-orange crude was purified by silica gel flash chromatography [gradient elution from 100% EtOAc to 90:10 EtOAc/MeOH(NH₃)] affording **17** (12.7 mg, yield 64%) as a yellow-orange glassy solid. ¹H NMR (400 MHz, MeOD) δ 7.58 (s, 1H, =CH), 7.45-7.39 (m, 1H, ArH), 6.90–6.83 (m, 2H, ArH), 4.14 (d, ⁴*J* = 2.4 Hz, 2H, -OCH₂C≡CH), 3.65–3.53 (m, 10H, -OCH₂), 3.50 (t, *J* = 6.5 Hz, 2H, -CONHCH₂), 2.81 (t, ⁴*J* = 2.4 Hz, 1H, ≡CH), 2.81–2.76 (bm, 4H, -NCH₂), 2.72 (q, *J* = 7.1 Hz, 2H, -NCH₂CH₃), 2.52 (s, 3H, CH₃), 2.49 (s, 3H, CH₃), 1.12 (t, *J* = 7.1 Hz, 3H, CH₃). ¹³C NMR (75 MHz, MeOD) δ 171.8 (Cq), 168.5 (Cq), 160.6 (d, ¹*J*_{CF} = 236 Hz, Cq), 138.3 (Cq), 136.0 (Cq), 131.7 (Cq), 128.8 (d, ³*J*_{CF} = 9 Hz, Cq), 127.6 (Cq), 125.5 (CH), 121.2 (Cq), 116.9 (Cq), 113.9 (d, ²*J*_{CF} = 25 Hz, CH), 111.3 (d, ³*J*_{CF} = 8 Hz, CH), 106.5 (d, ²*J*_{CF} = 26 Hz, CH), 80.7 (Cq), 76.1 (CH), 71.6 (CH₂), 71.5 (2C, CH₂), 71.5 (CH₂), 70.8 (CH₂), 70.2 (CH₂), 59.1 (CH₂), 54.0 (CH₂), 53.9 (CH₂), 49.7 (CH₂), 38.5 (CH₂), 13.7 (CH₃), 12.2 (CH₃), 11.1 (CH₃). HRMS (ES⁺) C₂₉H₃₇FN₄O₅ calcd for [M+H]⁺ 541.2821, found 541.2817.

Synthesis of compound 19. To a stirred suspension of **13** (7.7 mg, 0.026 mmol, 1.2 equiv) in dry DMF (200 μL), BOP (13.3 mg, 0.03 mmol, 1.4 equiv) and DIPEA (15 μL , 0.09 mmol, 4 equiv) were added and, after 5 min, a solution of **18** (11.7 mg, 0.21 mmol, 1 equiv) in dry DCM (200 μL) and dry DMF (100 μL) was added. The reaction mixture was left to stir under argon at room temperature for 16 h, protected from light. After reaction completion, the solvent was evaporated under reduced pressure and the residue was re-dissolved in EtOAc (2 mL) and the solution was washed with H₂O ($2 \times$) and saturated aqueous NaHCO₃ solution ($2 \times$). The organic layer was collected and concentrated under vacuum, affording an orange crude residue which was purified

1
2
3 by silica gel flash chromatography [EtOAc/MeOH(NH₃), 95:5] affording compound **19** (10.2
4 mg, yield 67%) as yellow glassy solid. ¹H NMR (400 MHz, MeOD) δ 7.47 (bs, 1H, =CH), 7.35
5 (m, 1H, H4 suni), 7.05 (d, ⁴J = 2.3 Hz, 2H, ArH), 6.86–6.80 (m, 2H, H6, H7 suni), 6.75 (t, J =
6 2.3 Hz, 1H, ArH), 4.74 (d, ⁴J = 2.3 Hz, 4H, ArOCH₂), 3.63–3.57 (m, 8H, -OCH₂), 3.52–3.44 (m,
7 4H, -CONHCH₂), 2.99 (t, ⁴J = 2.3 Hz, 2H, -≡CH), 2.77–2.69 (m, 6H, -NCH₂), 2.48 (s, 3H, CH₃),
8 2.43 (s, 3H, CH₃), 1.08 (t, ³J = 7.1 Hz, 3H, -NCH₂CH₃). ¹³C NMR (100 MHz, MeOD) δ 170.1
9 (Cq), 168.0 (Cq), 166.9 (Cq), 159.0 (d, ¹J_{CF} = 236.5 Hz, Cq), 158.8 (2C, Cq), 136.7 (Cq), 136.2
10 (Cq), 134.4 (Cq), 130.0 (Cq), 127.3 (d, ³J_{CF} = 9 Hz, Cq), 126.1 (Cq), 123.8 (CH), 119.5 (Cq),
11 115.3 (d, ⁴J_{CF} = 2.9 Hz, Cq), 112.3 (d, ²J_{CF} = 24.3 Hz, CH), 109.8 (d, ³J_{CF} = 8.5 Hz, CH), 106.6
12 (2C, CH), 104.9 (d, ²J_{CF} = 27.3 Hz, CH), 104.8 (CH), 78.0 (2C, Cq), 75.8 (2C, CH), 70.0 (CH₂),
13 69.9 (CH₂), 69.1 (CH₂), 69.0 (CH₂), 55.6 (2C, CH₂), 52.4 (2C, CH₂), 48.1 (CH₂), 39.5 (CH₂),
14 36.9 (CH₂), 12.2 (CH₃), 10.6 (CH₃), 9.6 (CH₃). HRMS (ES⁺) C₃₉H₄₄FN₅O₇ calcd for [M+H]⁺
15 714.3298, found 714.3290.
16
17
18
19
20
21
22
23
24
25
26
27
28
29
30
31
32
33
34

35 *Synthesis of the Sunitinib-c(AmpRGD) Conjugate 1.* A stirred solution of compounds **7** (20 mg,
36 0.02 mmol, 1 equiv) and **15** (12.8 mg, 0.03 mmol, 1.3 equiv) in dry DMF (2 mL) was degassed
37 at room temperature by argon/vacuum cycles (3 ×). To this solution was added a freshly prepared
38 aqueous mixture (1 mL) of Cu(OAc)₂ (1.39 mg, 0.007 mmol, 0.3 equiv) and sodium ascorbate
39 (2.8 mg, 0.014 mmol, 0.6 equiv), previously degassed by argon/vacuum cycles (3 ×). The
40 reaction mixture was degassed again and left to stir, protected from light, under argon at room
41 temperature for 20 h. After reaction completion, the mixture was concentrated under vacuum,
42 keeping the temperature under 50 °C. The crude was dissolved with 5 drops of MeOH, and a
43 yellow precipitate adhering to the round-bottom flask walls was obtained by means of the
44 dropwise addition of Et₂O and petroleum ether. The organic solvents were removed by a Pasteur
45
46
47
48
49
50
51
52
53
54
55
56
57
58
59
60

1
2
3
4
5
6
7
8
9
10
11
12
13
14
15
16
17
18
19
20
21
22
23
24
25
26
27
28
29
30
31
32
33
34
35
36
37
38
39
40
41
42
43
44
45
46
47
48
49
50
51
52
53
54
55
56
57
58
59
60

pipette. Subsequently, the residue was treated with water (3 ×), and the solvent was removed by a Pasteur pipette, affording a yellow-orange solid, which was used in the following step without further purification. The crude intermediate (30 mg, 0.02 mmol) was treated with a solution (1.2 mL) of TFA/TIS/H₂O (95:2.5:2.5) and the reaction mixture was left to stir for 2 h under argon at room temperature, protected from light. After solvent evaporation, the crude residue was washed thoroughly with Et₂O (4 ×) and petroleum ether (2 ×). Preparative RP-HPLC purification was performed [C₁₈-10 μm column, 21.2 × 250 mm; solvent A: H₂O (0.1% TFA) and solvent B: MeCN; flow rate 8.0 mL/min; detection 421 nm] using the following gradient elution: 0-1 min 5% B, 1-20 min 5-35% B, 20-28 min 35% B; *R*_t = 26.9 min. Product **1** (17.3 mg, yield 69%) was obtained as an orange glassy solid. [α]_D²⁵ = - 7.70 (*c* 1.0; MeOH). ¹H NMR (400 MHz, MeOD) δ 7.77 (s, 1H, ArH), 7.55 (s, 1H, =CH), 7.40 (m, 1H, ArH), 6.87 (m, 2H, ArH), 4.72 (t, *J* = 5.9 Hz, 1H, H α Asp), 4.53 (d, *J* = 11 Hz, 1H, H₂ Amp), 4.38 (t, *J* = 6.4 Hz, 2H, H1'), 4.31 (bm, 1H, H₄ Amp), 4.25 (t, *J* = 7.3 Hz, 1H, H α Arg), 4.08 (d, *J* = 13.6 Hz, 1H, H α Gly), 4.03 (m, 1H, H_{5a} Amp), 3.50 (m, 2H, H1'''), 3.47–3.40 (m, 3H, H2''' + H_{5b} Amp), 3.41 (d, *J* = 13.6 Hz, 1H, H α b Gly), 3.31–3.20 (m, 4H, H δ Arg + H₄'), 3.03 (t, *J* = 7.2 Hz, 2H, H₂''), 2.90 (m, 1H, H_{3a} Amp), 2.84 (d, *J* = 5.8 Hz, 2H, H β Asp), 2.71–2.56 (m, 3H, H_{3b} Amp + H1''), 2.48 (s, 3H, CH₃), 2.44 (s, 3H, CH₃), 2.02–1.86 (m, 2H, H₂'), 1.86–1.48 (m, 6H, H β Arg + H₃' + H γ Arg). ¹³C NMR (100 MHz, MeOD) δ 175.6 (Cq), 173.7 (Cq), 172.9 (Cq), 171.8 (Cq), 170.9 (Cq), 170.1 (Cq), 170.0 (Cq), 167.3 (Cq), 159.0 (d, ¹*J*_{CF} = 236 Hz, Cq), 157.3 (Cq), 146.6 (Cq), 136.7 (Cq), 134.4 (Cq), 130.1 (Cq), 127.2 (d, ³*J*_{CF} = 9 Hz, Cq), 126.1 (Cq), 123.7 (CH), 122.3 (CH), 119.4 (Cq), 115.3 (Cq), 112.3 (d, ²*J*_{CF} = 25 Hz, CH), 109.8 (d, ³*J*_{CF} = 8 Hz, CH), 104.8 (d, ²*J*_{CF} = 26 Hz, CH), 65.9 (CH), 60.3 (CH₂), 55.8 (CH), 54.6 (CH₂), 50.0 (CH), 49.7 (CH), 48.8 (CH₂), 44.5 (CH₂), 40.5 (CH₂), 39.0 (CH₂), 38.9 (CH₂), 34.9 (CH₂), 34.8 (CH₂), 34.7 (CH₂), 26.9 (CH₂), 26.5

(CH₂), 25.2 (CH₂), 22.3 (CH₂), 21.1 (CH₂), 12.1 (CH₃), 9.5 (CH₃). HRMS (ES⁺) C₄₄H₅₈FN₁₅O₉ calcd for [M+H]⁺ 960.4599, found 960.4576.

Synthesis of the Sunitinib-c(AmpRGD) Conjugate 2. Compound **2** was prepared according to the procedure described for the synthesis of compound **1**, starting from **7** (6.5 mg, 0.0076 mmol, 1 equiv) and **17** (5.3 mg, 0.0098 mmol, 1.3 equiv) in dry DMF (700 μL) and using Cu(OAc)₂ (0.45 mg, 0.002 mmol, 0.3 equiv), sodium ascorbate (0.9 mg, 0.0045 mmol, 0.6 equiv) in H₂O (300 μL). After 24 h, the protected intermediate (9 mg, 0.006 mmol) was treated with a solution of TFA/TIS/H₂O (321 μL). Preparative RP-HPLC purification was performed [C₁₈-10 μm column, 21.2 × 250 mm; solvent A: H₂O (0.1% TFA) and solvent B: MeCN, flow rate 8.0 mL/min; detection 421 nm] using the following gradient elution: 0-1 min 5% B, 1-20 min 5-35% B, 20-28 min 35% B; *R_t* = 26.4 min. Conjugate **2** (6.3 mg, as TFA salt, yield 70% for two steps) was obtained as yellow-orange glassy solid. [α]_D²⁰ = - 8.75 (*c* 0.16; MeOH). ¹H NMR (400 MHz, MeOD) δ 7.96 (s, 1H, CH triazole), 7.63 (s, 1H, =CH), 7.49–7.45 (m, 1H, ArH), 6.93–6.88 (m, 2H, ArH), 4.72 (t, *J* = 6.0 Hz, 1H, H_α Asp), 4.60 (s, 2H, -OCH₂-triazole), 4.56 (bd, *J* = 11 Hz, 1H, H₂ Amp), 4.43 (t, *J* = 6.0 Hz, 2H, H₁'), 4.30 (m, 1H, H₄ Amp), 4.24 (t, *J* = 7.2 Hz, 1H, H_α Arg), 4.11–4.00 (bm, 2H, H_{αa} Gly, H_{5a} Amp), 3.93–3.88 (m, 2H, -OCH₂), 3.80–3.73 (m, 2H, -CONHCH₂), 3.71–3.62 (m, 8H, -OCH₂), 3.55–3.36 (bm, 8H, -NCH₂, H_{αb} Gly, H_{5b} Amp), 3.31–3.22 (bm, 4H, H_δ Arg, H₄'), 2.97–2.82 (bm, 3H, H_{3a} Amp, H_β Asp), 2.68 (bd, *J* = 14.4 Hz, 1H, H_{3b} Amp), 2.55 (s, 3H, CH₃), 2.51 (s, 3H, CH₃), 2.01–1.91 (bm, 2H, H₂'), 1.86–1.58 (bm, 6H, H_β Arg, H₃', H_γ Arg), 1.41 (t, *J* = 7.2 Hz, 3H, CH₃). ¹³C NMR (100 MHz, MeOD) δ 175.7 (Cq), 172.8 (Cq), 171.8 (Cq), 170.9 (Cq), 170.3 (Cq), 170.1 (Cq), 168.7 (Cq), 159.1 (d, ¹*J*_{CF} = 236 Hz, Cq), 157.3 (Cq), 146.5 (Cq), 137.4 (Cq), 134.6 (Cq), 130.2 (Cq), 127.1 (d, ³*J*_{CF} = 9 Hz, Cq), 126.2 (Cq), 123.8 (2C, CH), 118.1 (Cq), 116.1 (Cq), 112.7 (d, ²*J*_{CF} = 25 Hz, CH), 110.0 (d, ³*J*_{CF}

1
2
3 = 9 Hz, CH), 105.2 (d, $^2J_{CF} = 26$ Hz, CH), 70.0 (2C, CH₂), 69.4 (2C, CH₂), 66.1 (CH), 64.3
4
5 (CH₂), 63.5 (CH₂), 60.2 (CH₂), 55.9 (CH), 54.7 (CH₂), 53.6 (CH₂), 52.7 (CH₂), 50.1 (CH), 49.7
6
7 (CH), 49.2 (CH₂), 48.9 (CH₂), 44.5 (CH₂), 40.5 (CH₂), 35.2 (CH₂), 34.7 (CH₂), 34.0 (CH₂), 26.9
8
9 (CH₂), 26.6 (CH₂), 25.2 (CH₂), 22.4 (CH₂), 12.4 (CH₃), 9.6 (CH₃), 7.9 (CH₃). HRMS (ES⁺)
10
11 C₅₀H₇₂FN₁₅O₁₁ calcd for [M+H]⁺ 1078.5593, found 1078.5585.
12
13
14
15

16 *Synthesis of the Sunitinib-c(AmpRGD) Conjugate 3.* Compound **3** was prepared according to the
17
18 procedure described for the synthesis of compound **1**, starting from **7** (28.1 mg, 0.033 mmol, 2.3
19
20 equiv) and **19** (10.2 mg, 0.014 mmol, 1 equiv) in dry DMF (2 mL) and using Cu(OAc)₂ (1.7 mg,
21
22 0.01 mmol, 0.6 equiv), sodium ascorbate (3.4 mg, 0.02 mmol, 1.2 equiv) in H₂O (0.9 mL). After
23
24 24 h, the protected intermediate (32.3 mg, 0.013 mmol) was treated with a solution of
25
26 TFA/TIS/H₂O (321 μL). Preparative RP-HPLC purification was performed [C₁₈-10 μm column,
27
28 21.2 × 250 mm; solvent A: H₂O (0.1% TFA) and solvent B: MeCN, flow rate 8.0 mL/min;
29
30 detection 421 nm] using the following gradient elution: 0-1 min 5% B, 1-23 min 5-40% B, 23-28
31
32 min 40% B; *R*_t = 21.8 min. Conjugate **3** (12.4 mg, as TFA salt, yield 43%) was obtained as a
33
34 yellow glassy solid. [α]_D²⁰ = -6.92 (c 0.39; MeOH). ¹H NMR (400 MHz, MeOD) δ 8.06 (s, 2H,
35
36 =CH triazole), 7.54 (s, 1H, =CH), 7.41 (m, 1H, H₄ suni), 7.07 (d, $^4J = 2.0$ Hz, 2H, ArH), 6.91–
37
38 6.86 (m, 2H, H₆ + H₇ suni), 6.70 (bt, $^4J = 2.0$ Hz, 1H, ArH), 5.21 (d, $^2J = 12.2$ Hz, 2H,
39
40 ArOCHa), 5.15 (d, $^2J = 12.2$ Hz, 2H, ArOCHb), 4.69 (t, *J* = 5.8 Hz, 2H, H_α Asp), 4.59 (bd, *J* =
41
42 10.6 Hz, 2H, H₂ Amp), 4.51–4.44 (m, 4H, H₁'), 4.33 (bs, 2H, H₄ Amp), 4.22 (bt, *J* = 6.6 Hz,
43
44 2H, H_α Arg), 4.13–4.01 (bm, 4H, H_{αα} Gly + H_{5a} Amp), 3.93–3.87 (bm, 2H, -OCH₂), 3.79–3.63
45
46 (bm, 8H, -CONHCH₂, -OCH₂), 3.60–3.38 (bm, 12H, -CONHCH₂, H_{ab} Gly, H_{5b} Amp + -NCH₂),
47
48 3.31 (bm, 4H, H_δ Arg), 3.26–3.21 (bm, 4H, H₄'), 3.00–2.88 (bm, 2H, H_{3a} Amp), 2.88–2.74 (m,
49
50 4H, H_β Asp), 2.73–2.65 (bd, *J* = 14.7 Hz, 2H, H_{3b} Amp), 2.50 (s, 3H, CH₃), 2.46 (s, 3H, CH₃),
51
52
53
54
55
56
57
58
59
60

1
2
3 2.04–1.92 (bm, 4H, H^{2'}), 1.84–1.57 (bm, 12H, H β Arg, H^{3'}, H γ Arg), 1.39 (t, $J = 7.2$ Hz, 3H, -
4 NCH₂CH₃). ¹³C NMR (100 MHz, MeOD) δ 175.6 (Cq), 172.8 (Cq), 171.8 (Cq), 171.0 (Cq),
5
6 170.2 (Cq), 169.9 (Cq), 168.7 (Cq), 168.4 (Cq), 159.4 (2C, Cq), 159.1 (d, $^1J_{CF} = 236.7$ Hz, Cq),
7
8 157.3 (2C, Cq), 143.5 (2C, Cq), 137.4 (Cq), 136.4 (Cq), 134.6 (Cq), 130.2 (Cq), 127.2 (d, $^3J_{CF} =$
9
10 9.1 Hz, Cq), 126.2 (Cq), 124.1 (2C, CH), 123.8 (CH), 118.0 (Cq), 115.9 (d, $^4J_{CF} = 2.9$ Hz, Cq),
11
12 112.6 (d, $^2J_{CF} = 24.0$ Hz, CH), 110.0 (d, $^3J_{CF} = 8.3$ Hz, CH), 106.3 (2C, CH), 105.1 (d, $^2J_{CF} =$
13
14 26.0 Hz, CH), 104.9 (CH), 70.2 (CH₂), 69.8 (CH₂), 69.1 (CH₂), 65.9 (2C, CH), 64.3 (CH₂), 61.2
15
16 (2C, CH₂), 60.5 (2C, CH), 55.9 (2C, CH), 54.6 (2C, CH₂), 52.7 (CH₂), 50.1 (2C, CH), 49.6 (2C,
17
18 CH), 49.1 (4C, CH₂), 44.6 (2C, CH₂), 40.5 (2C, CH₂), 39.5 (CH₂), 35.3 (CH₂), 34.9 (2C, CH₂),
19
20 34.7 (2C, CH₂), 26.9 (2C, CH₂), 26.5 (2C, CH₂), 25.2 (2C, CH₂), 22.4 (2C, CH₂), 12.4 (CH₃), 9.6
21
22 (CH₃), 7.9 (CH₃). HRMS (ES⁺) C₈₁H₁₁₄FN₂₇O₁₉ calcd for [M+2H]²⁺ 894.9457, found 894.9479.
23
24
25
26
27
28
29

30 **Biology.** All experimental procedures involving animals were performed in accordance with
31 national guidelines, approved by the ethical committee of Animal Welfare Office of Italian Work
32 Ministry (401/2015PR approved 05/21/2015) and conformed to the legal mandates and Italian
33 guidelines for the care and maintenance of laboratory animals.
34
35
36
37
38
39

40 **Cell Lines and Culture Conditions.** Endothelial progenitor cells (EPC) were kindly provided
41 by Prof. M. Del Rosso of the Department of Experimental and Clinical Biomedical Science,
42 University of Florence. Human umbilical cord blood (UCB) samples of health newborns were
43 used as a source of EPCs, as previously described.⁶³ EPCs were cultured on gelatin 1 %-coated
44 dishes in complete endothelial cell growth medium (EGM-2 BulletKit, Lonza), which includes
45 endothelial basal medium plus the SingleQuotes Kit (hydrocortisone, human fibroblast growth
46 factor B, VEGF, LongR3 insulin-like growth factor 1, ascorbic acid, human epidermal growth
47
48
49
50
51
52
53
54
55
56
57
58
59
60

1
2
3 factor, GA-1000, and heparin), supplemented with antibiotics (100 UI/mL penicillin, 100 lg/mL
4 streptomycin) and 10 % FBS. Cells were used between the third and tenth passages in vitro.
5
6
7

8
9 **In Vitro Plasma Stability.** Plasma was quickly thawed and diluted to 80% (v/v) with 100 mM
10 Phosphate Buffered Saline (PBS) pH 7.4 to control pH over the time period of the experiments.
11 Stock solutions of sunitinib and test compounds were added (final compound concentration: 1
12 μM) and maintained at 37 °C. At regular time points, aliquots of plasma solution were sampled,
13 two volumes of MeCN were added, samples were centrifuged (9,000 g, 10 min, 4 °C) and
14 analyzed by HPLC-UV-Vis for percentage of remaining compound over incubation time.
15
16
17
18
19
20
21
22

23
24 **Lipophilicity.** Distribution coefficients ($\text{Log } D_{\text{oct},7.4}$) values in the *n*-octanol/buffer partition
25 system for sunitinib and compounds **1-3** were measured at room temperature (25 ± 3 °C) by the
26 reference shake-flask method. Buffer was 50 mM MOPS (3-morpholinopropanesulfonic acid),
27 pH 7.4, with ionic strength adjusted to 0.15M for KCl addition. Test compounds, after
28 equilibrating for 4 h between pre-saturated partition phases under dark, were analyzed in each
29 phase by HPLC-UV-Vis, after dilution of each partition phase with MeOH. The $\text{Log } D_{\text{oct},7.4}$
30 values reported in Table are the means of at least three partition experiments employing different
31 *n*-octanol/buffer volume ratios.
32
33
34
35
36
37
38
39
40
41
42
43

44 **Cell Uptake.** Total intracellular concentrations of **1-3** and sunitinib were determined as
45 previously reported with minor modifications.⁶⁴ Briefly, EPCs were seeded in 6-well plates and
46 cultivated to confluence in complete medium. After 24 h, medium was replaced by fresh serum
47 and growth factor-free medium containing test compounds (sunitinib, **1-3**) at 1 μM
48 concentration. EPCs were incubated for 1 h at 37 °C and tested either immediately after or 8 h
49 after removal of the compound from the extracellular medium by washing the cells twice with 1
50
51
52
53
54
55
56
57
58
59
60

1
2
3 mL aliquots of PBS. Cell monolayers were next lysed and compounds were then extracted using
4
5 1 mL of absolute ethanol/well at 4 °C. Cell extracts were centrifuged (13000 rpm, 5 min, 4 °C) to
6
7 separate the supernatant which was then dried under nitrogen flow, dissolved in HPLC eluent
8
9 and injected into the HPLC-ESI-MS/MS system for quantification. Intracellular content of test
10
11 compounds was quantified as nmol compound/mg protein content in each sample. Cell pellets
12
13 were solubilized using 0.2 M NaOH for 5 min following the addition of the standard lysis buffer
14
15 and protein content was determined using the Bradford dye.
16
17
18
19

20
21 For specific displacement experiments, growing EP cells were detached from cultures by gentle
22
23 treatment with trypsin, washed, and resuspended in a serum-free medium and exposed to
24
25 conjugated compounds **2** and **3** or sunitinib at 1 μM concentration in the presence or in the
26
27 absence of compound **8** at 100 μM concentration. Cells were then incubated at 37 °C with 10%
28
29 CO₂ for 1 h. At the end of incubation, the cell suspensions were washed by centrifugation (1200
30
31 rpm, 5 min, 4 °C). Supernatants were discarded and ethanol extraction of the cell pellets was
32
33 performed at 4 °C for 10 min. Cell extracts were centrifuged (14000 rpm, 5 min, 4 °C) and
34
35 supernatants were evaporated under a stream of pure nitrogen for HPLC-ESI-MS/MS
36
37 quantification, as above.
38
39
40
41
42

43 **Cytofluorimetric assay.** Cells were detached by gentle treatment with Accutase (Lonza), a 0.5
44
45 mm EDTA solution, washed, and incubated for 1 h at 4 °C in the presence of anti- $\alpha_v\beta_3$
46
47 monoclonal antibody (1 μg/50 μL, anti-integrin $\alpha_v\beta_3$, clone LM609, Millipore). Cells were then
48
49 washed and incubated for 1 h at 4 °C with a specific secondary antibody, 5 mg/ml 1 μL/50 μL
50
51 goat antimouse IgG conjugated with fluorescein isothiocyanate (FITC; Santa Cruz Biotechnology,
52
53
54
55
56
57
58
59
60

1
2
3 Inc., SantaCruz, CA). Integrin-positive cells were analyzed at 488 nm using a FACScan system
4
5
6 flow cytometer (BD-FACS Canto).
7

8
9 **Solid-phase receptor binding assay.** Recombinant human integrin $\alpha_v\beta_3$ and $\alpha_5\beta_1$ receptors
10
11 (R&D Systems, Minneapolis, MN, USA) were diluted to 0.5 $\mu\text{g}/\text{mL}$ in coating buffer containing
12
13 20 mM Tris-HCl (pH 7.4), 150 mM NaCl, 1 mM MnCl_2 , 2 mM CaCl_2 , and 1 mM MgCl_2 . An
14
15 aliquot of diluted receptor (100 $\mu\text{L}/\text{well}$) was added to 96-well microtiter plates and incubated
16
17 overnight at 4 °C. The plates were incubated with blocking solution (coating buffer plus 1%
18
19 bovine serum albumin) for additional 2 h at room temperature to block nonspecific binding.
20
21 After washing 2 times with blocking solution, plates were incubated 3 h at room temperature, in
22
23 the dark, with various concentrations (10^{-5} – 10^{-12} M) of test compounds in the presence of 1
24
25 $\mu\text{g}/\text{mL}$ biotinylated vitronectin (for integrin $\alpha_v\beta_3$, vitronectin purchased from Molecular
26
27 Innovations, Novi, MI, USA) or biotinylated fibronectin (for integrin $\alpha_5\beta_1$, fibronectin purchased
28
29 from Sigma). Biotinylation was performed using an EZ-Link Sulfo-NHS-Biotinylation kit
30
31 (Pierce, Rockford, IL, USA). After washing 3 times, the plates were incubated for 1 h at room
32
33 temperature with streptavidin-biotinylated peroxidase complex (Amersham Biosciences,
34
35 Uppsala, Sweden). Plates were washed 3 times with blocking solution, followed by 30 min
36
37 incubation with 100 $\mu\text{L}/\text{well}$ Substrate Reagent Solution (R&D Systems, Minneapolis, MN,
38
39 USA) before stopping the reaction with the addition of 50 $\mu\text{L}/\text{well}$ 2N H_2SO_4 . Absorbance at 415
40
41 nm was read in a SynergyTM HT Multi-Detection Microplate Reader (BioTek Instruments,
42
43 Inc.). Each data point represents the average of triplicate wells; data analysis was carried out by
44
45 nonlinear regression analysis with GraphPad Prism software. Each experiment was repeated in
46
47
48
49
50
51
52
53
54
55
56
57
58
59
60 duplicate.

1
2
3
4
5
6
7 **Cell-adhesion assay.** Plates (96 wells) were coated with vitronectin (10 mg/mL) by overnight
8
9 incubation at 4 °C. Plates were washed with phosphate buffer solution (PBS) and then incubated
10
11 at 37 °C for 1 h with PBS/1% BSA. After being washed, EPCs were counted and resuspended in
12
13 serum-free medium, then exposed to the compound (final concentration was 1, 10, 100, 1000,
14
15 10000 nM) at 37 °C for 30 min to allow the ligand–receptor equilibrium to be reached. Assays
16
17 were performed in the presence of 2.0 mmol/L MnCl₂. Cells were then plated (5-6×10⁴ cells per
18
19 well) and incubated at 37 °C for 1 h. All the wells were washed with PBS to remove the non-
20
21 adherent cells, and 0.5% crystal violet solution in 20% methanol was added. After 2 h of
22
23 incubation at 4 °C, plates were examined at 540 nm using a counter ELX800 (Bio TEK
24
25 Instruments). Experiments were conducted in triplicate and were repeated at least three times.
26
27 The values are expressed as percentage inhibition ±SEM (standard error of mean) of cell
28
29 adhesion relative to untreated cells.
30
31
32
33
34
35

36 **Cell proliferation.** EPCs were seeded on gelatin-coated 24-well plates at 6,000 cells/well. After
37
38 4 h adhesion in complete medium, cells were exposed to a serum-free medium supplemented
39
40 with 20 ng/mL VEGFA containing different compounds at 1 μM concentration. After 24 h, 48 h
41
42 and 72 h, cell numbers and cell viability were determined using trypan blue exclusion assay. All
43
44 assays were performed in triplicate and repeated at least three times.
45
46
47
48

49 **In vitro kinase assay.** Evaluation of the effects of compound **3** on the kinase activity of human
50
51 recombinant PDGFRβ and VEGFR2 was performed by measuring the phosphorylation of the
52
53 substrates Ulight-PolyGAT[EAY(1:1:1)]_n or Ulight-CAGAGAIETDKEYYTVKD (JAK1),
54
55
56
57
58
59
60

1
2
3 respectively, using human recombinant enzymes and the LANCE detection method,⁶⁵ employing
4
5 the Cerep kinase assays.⁶⁶
6
7

8
9 **Western blotting analysis.** EPCs were grown in standard condition for 24 h and then exposed to
10
11 different compounds at 1 μ M concentration in a serum and growth factor free medium. After 1 h
12
13 incubation, cells were treated with 20 ng/mL VEGF-A for 5 min. Next, EPCs were washed twice
14
15 with ice cold PBS containing 1 mM Na_4VO_3 , and lysed in 100 μ L of RIPA lysis buffer (#20-188,
16
17 Millipore) containing 100 μ M PMSF and 100 μ M OVA and protease inhibitor cocktail-I (#20-
18
19 201, Millipore). Aliquots of supernatants containing equal amounts of protein in LDS sample
20
21 buffer (iBlot) were separated on 4-12% (Bis-Tris Plus Blot, Invitrogen). Transfer of fractionated
22
23 proteins from the gel to a PVDF membrane (iBlot PVDF, Invitrogen) was performed using iBlot
24
25 system (Invitrogen). Membranes were then blocked with Fluorescent Blocker (Millipore) 1:1
26
27 diluted in PBS for 1 h at room temperature. Subsequently, the membrane was probed at 4 $^{\circ}\text{C}$
28
29 overnight with 1:1000 rabbit anti-phosphotyrosine-VEGFR2 (#2471 anti-pTyr951, Cell
30
31 Signaling) or with 1:1000 rabbit anti-VEGFR2 (#441053G, Invitrogen). The membrane was
32
33 washed in T-PBS buffer, and incubated for 1 h at room temperature with goat anti-rabbit IgG
34
35 Alexa Flour 750 antibodies (Invitrogen). Immunoreactive bands were visualized by an Odyssey
36
37 Infrared Imaging System (LI-COR Bioscience). Mouse anti-alpha-tubulin mouse monoclonal
38
39 antibody (Sigma)/goat anti-mouse IgG Alexa Flour 680 antibodies (Invitrogen), were used to
40
41 assess equal amount of protein loaded in each lane.
42
43
44
45
46
47
48
49

50 **In vitro angiogenesis assay.** The effects of the different compounds on the ability of EPCs to
51
52 reorganize and differentiate into capillary-like network were assessed by Matrigel
53
54 morphogenesis assay. Briefly, 50 μ L of Matrigel matrix growth factor reduced (0.96 mg/mL)
55
56
57
58
59
60

1
2
3 was added into wells of a 96-well plate and polymerized for 1 h at 37 °C. Endothelial cells, after
4
5 24 h of incubation in standard EGM-2 medium, were washed once with PBS, harvested by
6
7 trypsinization, and collected by centrifugation. Then, cells were resuspended in 200 µL of
8
9 serum/growth factor free EGM-2 medium containing VEGF-A (20ng/mL) and different
10
11 concentrations of compounds and placed into Matrigel-coated wells (7×10^4 EPC/well). Cells
12
13 diluted in EGM- 2 basal medium supplemented with VEGF 20 ng/mL were used as positive
14
15 control. After 6 h incubation on Matrigel at 37 °C, the plates were photographed under a phase
16
17 contrast microscope and the degree of tubule formation was quantified. The honeycomb pattern
18
19 is the combination of a series of nodes connected together by branches surrounding enclosed
20
21 tissues (meshes or loops), thus for quantification of capillary network, the number of loops in
22
23 four randomly chosen fields from each well was counted. Each experiment was carried out in
24
25 triplicate.
26
27
28
29
30
31
32

33 **In vivo angiogenesis assay.** Female FVB mice were subcutaneously implanted in both flanks
34
35 with 0.4 mL of the EHS-derived basement membrane matrix Matrigel (BD Bioscience) which
36
37 contains types IV collagen, proteoglycans and laminin. Matrigel plugs were added with heparin
38
39 (5000 U/mL) and VEGF-A (50 ng/mL). Mice were i.p injected every day with 10 mg/kg of
40
41 sunitinib alone, or equivalent quantity within compound **8**, sunitinib plus **8**, or compound **3**.
42
43 After 4 days, mice were sacrificed, Matrigel plugs were removed and processed for microscopy
44
45 investigations.
46
47
48
49
50
51
52
53

54 ASSOCIATED CONTENT
55
56
57
58
59
60

1
2
3 **Supporting Information Available:** Synthesis of linkers, sunitinib and peptide intermediates
4
5 and c(AmpRGD)-fluorescein conjugate, HPLC-UV-Vis, HPLC-ESI-MS/MS, flow
6
7 cytofluorimetry, cell uptake studies, ¹H NMR spectra of compounds **1-3**, molecular formula
8
9 strings. This material is available free of charge via the Internet at <http://pubs.acs.org>.
10
11

12 AUTHOR INFORMATION

13 14 15 **Corresponding Authors**

16
17
18
19 * For F. B.: phone, 00390552751310; e-mail: francesca.bianchini@unifi.it
20
21

22
23 *For F. Z.: phone, 00390521905067; e-mail: franca.zanardi@unipr.it
24
25

26 **Author Contributions**

27
28 The manuscript was written through contributions of all authors. All authors have given approval
29
30 to the final version of the manuscript.
31
32

33 ACKNOWLEDGMENTS

34
35
36
37 A.S., E.P., L.B., D.A., F.B., F.Z. received funding from Ministero dell'Istruzione,
38
39 dell'Università e della Ricerca (MIUR, PRIN 2010–2011, Protocol No. 2010NRREPL_006);
40
41 L.C., A.P., F.B. received funding from the Istituto Toscano Tumori (ITT) (Grant No. 7197
42
43 29/12/2009) and Ente Cassa di Risparmio di Firenze (Protocol No. 2013.0688). Thanks are due
44
45 to Dr. Valentina Beatrizzotti and Dr. Miriam Girardini (University of Parma) for some synthesis
46
47 experiments.
48
49
50

51 ABBREVIATIONS

52
53
54
55
56
57
58
59
60

1
2
3 Amp, 4-amino-L-proline; Boc, *tert*-butoxycarbonyl; Pmc, 2,2,5,7,8-pentamethylchroman-6-
4 sulfonyl; Fmoc, 9-fluorenylmethoxycarbonyl; SPPS, solid phase peptide synthesis; 1,2-DCE,
5 1,2-dichloroethane; DCM, dichloromethane; DMF, *N,N*-dimethylformamide; DIPEA,
6 diisopropylethylamine; TFA, trifluoroacetic acid; TFE, trifluoroethanol; HATU, *O*-(7-
7 azabenzotriazol-1-yl)-*N,N,N',N'*-tetramethyluronium hexafluorophosphate; HOAt, 1-hydroxy-7-
8 azabenzotriazole; BOP, (benzotriazol-1-yloxy)tris(dimethylamino)phosphonium
9 hexafluorophosphate; TIS, triisopropylsilane; DMAP, 4-(dimethylamino)pyridine; Na L-Asc,
10 (+)-sodium L-ascorbate.
11
12
13
14
15
16
17
18
19
20
21
22
23
24
25

26 REFERENCES

- 27
28 1. Lammers, T.; Kiessling, F.; Hennink, W. E.; Storm, G. Drug targeting to tumors:
29 principles, pitfalls and (pre-)clinical progress. *J. Control. Release* **2012**, *161*, 175-187.
30
31
- 32 2. Svensen, N.; Walton, J. G. A.; Bradley, M. Peptides for cell-selective drug delivery.
33 *Trends Pharmacol. Sci.* **2012**, *33*, 186-192.
34
35
- 36 3. Krall, N.; Scheuermann, J.; Neri, D. Small targeted cytotoxics: current state and promises
37 from DNA-encoded chemical libraries. *Angew. Chem. Int. Ed.* **2013**, *52*, 1384-1402.
38
39
- 40 4. Hopkins, A. L. Network pharmacology: the next paradigm in drug discovery. *Nat. Chem.*
41 *Biol.* **2008**, *4*, 682-690.
42
43
- 44 5. Dar, A. C.; Das, T. K.; Shokat, K. M.; Cagan, R. L. Chemical genetic discovery of targets
45 and anti-targets for cancer polypharmacology. *Nature* **2012**, *486*, 80-84.
46
47
- 48 6. Daydé-Cazals, B.; Fauvel, B.; Singer, M.; Feneyrolles, C.; Bestgen, B.; Gassiot, F.;
49 Spenlinhauer, A.; Warnault, P.; Van Hijfte, N.; Borjini, N.; Chev e, G.; Yasri, A. Rational
50
51
52
53
54
55
56
57
58
59
60

- 1
2
3 design, synthesis, and biological evaluation of 7-azaindole derivatives as potent focused
4 multi-targeted kinase inhibitors. *J. Med. Chem.* **2016**, *59*, 3886-3905.
5
6
7
8 7. Hanahan, D.; Folkman, J. Patterns and emerging mechanisms of the antiangiogenic
9 switch during tumorigenesis. *Cell* **1996**, *86*, 353-364.
10
11
12 8. Ferrara, N.; Kerbel, R. S. Angiogenesis as a therapeutic target. *Nature* **2005**, *438*, 967-
13 974.
14
15
16
17 9. Folkman, J. Angiogenesis: an organizing principle for drug discovery? *Nat. Rev. Drug*
18 *Discov.* **2007**, *6*, 273-286.
19
20
21
22 10. Weis, S. M.; Chesh, D. A. Tumor angiogenesis: molecular pathways and therapeutic
23 targets. *Nat. Med.* **2011**, *17*, 1359-1370.
24
25
26
27 11. Carmeliet, P.; Jain, R. K. Molecular mechanisms and clinical applications of
28 angiogenesis. *Nature* **2011**, *473*, 298-307.
29
30
31
32 12. Prokopiou, E. M.; Ryder, S. A.; Walsh, J. J. Tumour vasculature targeting agents in
33 hybrid/conjugate drugs. *Angiogenesis* **2013**, *16*, 503-524.
34
35
36
37 13. Sun, L.; Liang, C.; Shirazian, S.; Zhou, Y.; Miller, T.; Cui, J.; Fukuda, J. Y.; Chu, J.-Y.;
38 Nematalla, A.; Wang, X.; Chen, H.; Sistla, A.; Luu, T. C.; Tang, F.; Wei, J.; Tang, C.
39 Discovery of 5-[5-fluoro-2-oxo-1,2-dihydroindol-(3*Z*)-ylidenemethyl]-2,4-dimethyl-1*H*-
40 pyrrole-3-carboxylic acid (2-diethylaminoethyl)amide, a novel tyrosine kinase inhibitor
41 targeting vascular endothelial and platelet-derived growth factor receptor tyrosine kinase.
42
43
44
45
46
47
48 *J. Med. Chem.* **2003**, *46*, 1116-1119.
49
50
51 14. Faivre, S.; Demetri, G.; Sargent, W.; Raymond, E. Molecular basis for sunitinib efficacy
52 and future clinical development. *Nat. Rev. Drug Discov.* **2007**, *6*, 734-745.
53
54
55
56
57
58
59
60

- 1
2
3
4
5
6
7
8
9
10
11
12
13
14
15
16
17
18
19
20
21
22
23
24
25
26
27
28
29
30
31
32
33
34
35
36
37
38
39
40
41
42
43
44
45
46
47
48
49
50
51
52
53
54
55
56
57
58
59
60
15. Raymond, E.; Dahan, L.; Raoul, J.-L.; Bang, Y.-J.; Borbath, I.; Lomabrd-Bohas, C.; Valle, J.; Metrakos, P.; Smith, D.; Vinik, A.; Chen, J.-S.; Hörsch, D.; Hammel, P.; Wiedenmann, B.; Van Cutsem, E.; Patyna, S.; Lu, D. R.; Blanckmeister, C.; Chao, R.; Ruzzniewski, P. Sunitinib malate for the treatment of pancreatic neuroendocrine tumors. *N. Engl. J. Med.* **2011**, *364*, 501-513.
16. Bagchi, S. Sunitinib still first-line therapy for metastatic renal cancer. *Lancet Oncol.* **2014**, *15*, e420.
17. NIH clinical trials of sunitinib: <https://clinicaltrials.gov/ct2/> (August 22, 2016). Very recently, sunitinib was found to be a potent acetylcholinesterase (AChE) inhibitor with activity in attenuating cognitive impairments in mice. See: Huang, L.; Lin, J.; Xiang, S.; Zhao, K.; Yu, J.; Zheng, J.; Xu, D.; Nirasha, S.; Wang, C.; Chen, X.; Zhang, J.; Xu, S.; Wei, X.; Zhang, Z.; Zhou, D.; Han, Y.; Zhou, W.; Cui, W.; Hu, Z.; Wang, Q. Sunitinib, a clinically anticancer drug, is a potent AChE inhibitor and attenuates cognitive impairments in mice. *ACS Chem Neurosci.* **2016**, *7*, 1047-1056.
18. Mas-Moruno, C.; Rechenmacher, F.; Kessler, H. Cilengitide: the first anti-angiogenic small molecule drug candidate. Design, synthesis and clinical evaluation. *Anti-Cancer Agents Med. Chem.* **2010**, *10*, 753-768.
19. Stupp, R.; Hegi, M. E.; Gorlia, T.; Erridge, S. C.; Perry, J.; Hong, Y.-K.; Aldape, K. D.; Lhermitte, B.; Pietsch, T.; Grujicic, D.; Steinbach, J. P.; Wick, W.; Tarnawski, R.; Nam, D.-H.; Hau, P.; Weyerbrock, A.; Taphoorn, M. J. B.; Shen, C.-C.; Rao, N.; Thurzo, L.; Herrlinger, U.; Gupta, T. Cilengitide combined with standard treatment for patients with newly diagnosed glioblastoma with methylated MGMT promoter (CENTRIC EORTC

- 1
2
3 26071-22072 study): a multicenter, randomized, open-label, phase 3 trial. *Lancet Oncol.*
4
5 **2014**, *15*, 1100-1108.
6
7
8 20. O'Donnel, P. H.; Karovic, S.; Karrison, T. G.; Janisch, L.; Levine, M. R.; Harris, P. J.;
9
10 Polite, B. N.; Cohen, E. E. W.; Fleming, G. F.; Ratain, M. J.; Maitland, M. L. Serum C-
11
12 telopeptide collagen crosslinks and plasma soluble VEGFR2 as pharmacodynamics
13
14 biomarkers in a trial of sequentially administered sunitinib and cilengitide. *Clin. Cancer*
15
16 *Res.* **2015**, *21*, 5092-5099.
17
18
19 21. Vansteenkiste, J.; Barlesi, F.; Waller, C. F.; Bennouna, J.; Gridelli, C.; Goekkurt, E.;
20
21 Verhoeven, D.; Szczesna, A.; Feurer, M.; Milanowski, J.; Germonpre, P.; Lena, H.;
22
23 Atanackovic, D.; Krzakowski, M.; Hickling, C.; Straub, J.; Picard, M.; Schuette, W.;
24
25 O'Byrne, K. Cilengitide combined with cetuximab and platinum-based chemotherapy as
26
27 first-line treatment in advanced non-small-cell lung cancer (NSCLC) patients: results of
28
29 an open-label, randomized, controlled phase II study (CERTO). *Ann. Oncol.* **2015**, *26*,
30
31 1734-1740.
32
33
34 22. Jain, R. K. Antiangiogenesis strategies revisited: from starving tumors to alleviating
35
36 hypoxia. *Cancer Cell* **2014**, *26*, 605-622.
37
38
39 23. [https://www.uptodate.com/contents/toxicity-of-molecularly-targeted-antiangiogenic-](https://www.uptodate.com/contents/toxicity-of-molecularly-targeted-antiangiogenic-agents-cardiovascular-effects)
40
41 [agents-cardiovascular-effects](https://www.uptodate.com/contents/toxicity-of-molecularly-targeted-antiangiogenic-agents-cardiovascular-effects) (August 22, 2016).
42
43
44 24. [https://www.uptodate.com/contents/toxicity-of-molecularly-targeted-antiangiogenic-](https://www.uptodate.com/contents/toxicity-of-molecularly-targeted-antiangiogenic-agents-non-cardiovascular-effects)
45
46 [agents-non-cardiovascular-effects](https://www.uptodate.com/contents/toxicity-of-molecularly-targeted-antiangiogenic-agents-non-cardiovascular-effects) (August 22, 2016).
47
48
49 25. Bergers, G.; Hanahan, D. Modes of resistance to anti-angiogenic therapy. *Nat. Rev.*
50
51 *Cancer* **2008**, *8*, 592-603.
52
53
54
55
56
57
58
59
60

- 1
2
3
4 26. Francia, G.; Emmenegger, U.; Kerbel, R. S. Tumor-associated fibroblasts as “Trojan
5
6 horse” mediators of resistance to anti-VEGF therapy. *Cancer Cell* **2009**, *15*, 3-5.
7
- 8 27. Ebos, J. M. L.; Lee, C. R.; Cruz-Munoz, W.; Bjarnason, G. A.; Christensen, J. G.; Kerbel,
9
10 R. S. Accelerated metastasis after short-term treatment with a potent inhibitor of tumor
11
12 angiogenesis. *Cancer Cell* **2009**, *15*, 232-239.
13
- 14 28. Gotink, K. J.; Broxterman, H. J.; Labots, M.; de Haas, R. R.; Dekker, H.; Honeywell, R.
15
16 J.; Rudek, M. A.; Beerepoot, L. V.; Musters, R. J.; Jansen, G.; Griffioen, A. W.; Assaraf,
17
18 Y. G.; Pili, R.; Peters, G. J.; Verheul, H. M. W. Lysosomal sequestration of sunitinib: a
19
20 novel mechanism of drug resistance. *Clin. Cancer Res.* **2011**, *17*, 7337-7346.
21
22
- 23 29. Gacche, R. N. Compensatory angiogenesis and tumor refractoriness. *Oncogenesis* **2015**,
24
25 *4*, e153.
26
27
- 28 30. El-Kenawi, A. E.; El-Remessy, A. B. Angiogenesis inhibitors in cancer therapy:
29
30 mechanistic perspective on classification and treatment rationales. *Brit. J. Pharmacol.*
31
32 **2013**, *170*, 712-729.
33
34
- 35 31. Reynolds, A. R.; Reynolds, L. E.; Nagel, T. E.; Lively, J. C.; Robinson, S. D.; Hicklin, D.
36
37 J.; Bodary, S. C.; Hodivala-Dilke, K. M. Elevated Flk1 (vascular endothelial growth
38
39 factor receptor 2) signaling mediates enhanced angiogenesis in beta3-integrin-deficient
40
41 mice. *Cancer Res.* **2004**, *64*, 8643-8650.
42
43
44
- 45 32. Mahabeleshwar, G. H.; Feng, W.; Phillips, D. R.; Byzova, T. V. Integrin signaling is
46
47 critical for pathological angiogenesis. *J. Exp. Med.* **2006**, *203*, 2495-2507.
48
49
- 50 33. Mahabeleshwar, G. H.; Feng, W.; Reddy, K.; Plow, E. F.; Byzova, T. V. Mechanisms of
51
52 integrin-vascular endothelial growth factor receptor cross-activation in angiogenesis.
53
54 *Circ. Res.* **2007**, *101*, 570-580.
55
56
57
58
59
60

- 1
2
3
4
5
6
7
8
9
10
11
12
13
14
15
16
17
18
19
20
21
22
23
24
25
26
27
28
29
30
31
32
33
34
35
36
37
38
39
40
41
42
43
44
45
46
47
48
49
50
51
52
53
54
55
56
57
58
59
60
34. Mahabeleshwar, G. H.; Chen, J.; Feng, W.; Somanath, P. R.; Razorenova, O. V.; Byzova, T. V. Integrin affinity modulation in angiogenesis. *Cell Cycle* **2008**, *7*, 335-347.
35. Somanath, P. R.; Malinin, N. L.; Byzova, T. V. Cooperation between integrin $\alpha_v\beta_3$ and VEGFR2 in angiogenesis. *Angiogenesis* **2009**, *12*, 177-185.
36. Robinson, S. D.; Hodivala-Dilke, K. M. The role of β_3 -integrins in tumor angiogenesis: context is everything. *Curr. Opin. Cell Biol.* **2011**, *23*, 630-637.
37. Strieth, S.; Eichhorn, M. E.; Sutter, A.; Jonczyk, A.; Berghaus, A.; Dellian, M. Antiangiogenic combination tumor therapy blocking α_v -integrins and VEGF-receptor-2 increases therapeutic effects *in vivo*. *Int. J. Cancer* **2006**, *119*, 423-431.
38. Papo, N.; Silverman, A. P.; Lahti, J. L.; Cochran, J. R. Antagonistic VEGF variants engineered to simultaneously bind to and inhibit VEGFR2 and $\alpha_v\beta_3$ integrin. *Proc. Natl. Acad. Sci. U.S.A.* **2011**, *108*, 14067-14072.
39. Kim, T. J.; Landen, C. N.; Lin, Y. G.; Mangal, L. S.; Lu, C.; Nick, A. M.; Stone, R. L.; Merritt, W. M.; Armaiz-Pena, G.; Jennings, N. B.; Coleman, R. L.; Tice, D. A.; Sood, A. K. Combined anti-angiogenic therapy against VEGF and integrin $\alpha_v\beta_3$ in an orthotopic model of ovarian cancer. *Cancer Biol. Ther.* **2009**, *8*, 2261-2270.
40. Zanella, S.; Mingozzi, M.; Dal Corso, A.; Fanelli, R.; Arosio, D.; Cosentino, M.; Schembri, L.; Marino, F.; De Zotti, M.; Formaggio, F.; Pignataro, L.; Belvisi, L.; Piarulli, U.; Gennari, C. Synthesis, characterization, and biological evaluation of a dual-action ligand targeting $\alpha_v\beta_3$ integrin and VEGF receptors. *ChemistryOpen* **2015**, *4*, 633-641.
41. Zanardi, F.; Burreddu, P.; Rassu, G.; Auzzas, L.; Battistini, L.; Curti, C.; Sartori, A.; Nicastro, G.; Menchi, G.; Cini, N.; Bottoncetti, A.; Raspanti, S.; Casiraghi, G. Discovery of subnanomolar arginine-glycine-aspartate-based $\alpha_v\beta_3/\alpha_v\beta_5$ integrin binders embedding

- 1
2
3 4-aminoproline residues. *J. Med. Chem.* **2008**, *51*, 1771-1782 (corrigendum *J. Med.*
4
5 *Chem.* **2008**, *51*, 2870).
6
7
- 8 42. Battistini, L.; Burreddu, P.; Carta, P.; Rassu, G.; Auzzas, L.; Curti, C.; Zanardi, F.;
9
10 Manzoni, L.; Araldi, E. M. V.; Scolastico, C.; Casiraghi, G. 4-Aminoproline-based
11
12 arginine-glycine-aspartate integrin binders with exposed ligation points: practical in-
13
14 solution synthesis, conjugation and binding affinity evaluation. *Org. Biomol. Chem.*
15
16 **2009**, *7*, 4924-4935.
17
18
- 19 43. Sartori, A.; Bianchini, F.; Migliari, S.; Burreddu, P.; Curti, C.; Vacondio, F.; Arosio, D.;
20
21 Ruffini, L.; Rassu, G.; Calorini, L.; Pupi, A.; Zanardi, F.; Battistini, L. Synthesis and
22
23 preclinical evaluation of a novel, selective ¹¹¹In-labelled aminoproline-RGD-peptide for
24
25 non-invasive melanoma tumor imaging. *Med. Chem. Commun.* **2015**, *6*, 2175-2183.
26
27
28
- 29 44. For an example of cell-selective sunitinib-like/platinum(II) bioconjugate with multikinase
30
31 inhibitory activity, see: Harmsen, S.; Dolman, M. E. M.; Nemes, Z.; Lacombe, M.;
32
33 Szokol, B.; Pató, J.; Kéri, G.; Orfi, L.; Storm, G.; Hennink, W. E.; Kok, R. J.
34
35 Development of a cell-selective and intrinsically active multikinase inhibitor
36
37 bioconjugate. *Bioconj. Chem.* **2011**, *22*, 540-545.
38
39
- 40 45. For an example of targeted liposome-mediated delivery of sunitinib, see: Shi, J.-F.; Sun,
41
42 M.-G.; Li, X.-Y.; Zhao, Y.; Ju, R.-J.; Mu, L.-M.; Yan, Y.; Li, X.-T.; Zeng, F.; Lu, W.-L.
43
44 A combination of targeted sunitinib liposomes and targeted vinorelbine liposomes for
45
46 treating invasive breast cancer. *J. Biomed. Nanotech.* **2015**, *11*, 1568-1582.
47
48
- 49 46. Very recently, the synthesis and preclinical studies of one GnRH-sunitinib succinate-
50
51 linked conjugate was reported, which was proven to selectively reach prostate cancer site
52
53 and downregulate angiogenesis. See: Argyros, O.; Karampelas, T.; Asvos, X.; Varela, A.;
54
55
56
57
58
59
60

- 1
2
3 Sayyad, N.; Papakyriakou, A.; Davos, C. H.; Tzakos, A. G.; Fokas, D.; Tamvakopoulos,
4 C. Peptide-drug conjugate GnRH-sunitinib targets angiogenesis selectively at the site of
5 action to inhibit tumor growth. *Cancer Res.* **2016**, *76*, 1181-1192.
6
7
8
9
10
11 47. Musumeci, F.; Radi, M.; Brullo, C.; Schenone, S. Vascular endothelial growth factor
12 (VEGF) receptors: drugs and new inhibitors. *J. Med. Chem.* **2012**, *55*, 10797-10822.
13
14
15 48. McTigue, M.; Murray, B. W.; Chen, J. C.; Deng, Y.-L.; Solowiej, J.; Kania, R. S.
16 Molecular conformations, interactions, and properties associated with drug efficiency and
17 clinical performance among VEGFR TK inhibitors. *Proc. Natl. Acad. Sci.* **2012**, *109*,
18 18281-18289.
19
20
21
22
23
24 49. Capelli, A. M.; Costantino, G. Unbinding pathways of VEGFR2 inhibitors revealed by
25 steered molecular dynamics. *J. Chem. Inf. Model.* **2014**, *54*, 3124-3136.
26
27
28
29 50. Pilkington-Miksa, M.; Arosio, D.; Battistini, L.; Belvisi, L.; De Matteo, M.; Vasile, F.;
30 Burreddu, P.; Carta, P.; Rassu, G.; Perego, P.; Carenini, N.; Zunino, F.; De Cesare, M.;
31 Castiglioni, V.; Scanziani, E.; Scolastico, C.; Casiraghi, G.; Zanardi, F.; Manzoni L.
32 Design, synthesis and biological evaluation of novel cRGD-paclitaxel conjugates for
33 integrin-assisted drug delivery. *Bioconj. Chem.* **2012**, *23*, 1610-1622.
34
35
36
37
38
39 51. Battistini, L.; Burreddu, P.; Sartori, A.; Arosio, D.; Manzoni, L.; Paduano, L.; D'Errico,
40 G.; Sala, R.; Reia, L.; Bonomini, S.; Rassu, G.; Zanardi, F. Enhancement of the uptake
41 and cytotoxic activity of doxorubicin in cancer cells by novel cRGD-semipeptide-
42 anchoring liposomes. *Mol. Pharm.* **2014**, *11*, 2280-2293.
43
44
45
46
47
48
49 52. Boturyn, D.; Coll, J.-L.; Garanger, E.; Favrot, M.-C.; Dumy, P. Template assembled
50 cyclopeptides as multimeric system for integrin targeting and endocytosis. *J. Am. Chem.*
51 *Soc.* **2004**, *126*, 5730-5739.
52
53
54
55
56
57
58
59
60

- 1
2
3
4 53. Dijkgraaf, I.; Kruijtzter, J. A.; Liu, S.; Soede, A. C.; Oyen, W. J. G.; Corstens, F. H.;
5
6 Liskamp, R. M.; Boerman, O. C. Improved targeting of the $\alpha_v\beta_3$ integrin by
7
8 multimerization of RGD peptides. *Eur. J. Nucl. Med. Mol. Imaging* **2007**, *34*, 267-273.
9
10
11 54. Liu, S. Radiolabeled RGD peptides as integrin $\alpha_v\beta_3$ -targeted radiotracers: maximizing
12
13 binding affinity via bivalency. *Bioconj. Chem.* **2009**, *20*, 2199-2213.
14
15
16 55. Sancey, L.; Garanger, E.; Foillard, S.; Schoehn, G.; Hurbin, A.; Albiges-Rizo, C.;
17
18 Boturyn, D.; Souchier, C.; Grichine, A.; Dumy, P.; Coll, J.-L. Clustering and
19
20 internalization of integrin $\alpha_v\beta_3$ with a tetrameric RGD-synthetic peptide. *Mol. Ther.*
21
22 **2009**, *17*, 837-843.
23
24
25 56. Ivaska, J.; Heino, J. Cooperation between integrins and growth factor receptors in
26
27 signaling and endocytosis. *Annu. Rev. Cell Dev. Biol.* **2011**, *27*, 291-320.
28
29
30 57. Liu, S. Radiolabeled cyclic RGD peptide bioconjugates as radiotracers targeting multiple
31
32 integrins. *Bioconj. Chem.* **2015**, *26*, 1413-1438.
33
34
35 58. The photoinduced *Z-E* isomerization of sunitinib drug is reknown as it is known that dark
36
37 conditions promote reversible re-conversion to the biologically active *Z*-isomer. In our
38
39 hands, all “sunitinib-containing” compounds were pure *Z*-configured compounds and
40
41 were treated under dark conditions to prevent possible isomerization. See: Sistla, A.;
42
43 Shenoy, N. Reversible *Z-E* isomerism and pharmaceutical implications for SU5416. *Drug*
44
45 *Dev. Ind. Pharm.* **2005**, *31*, 1001-1007.
46
47
48 59. Ribatti, D. The involvement of endothelial progenitor cells in tumor angiogenesis. *J. Cell*
49
50 *Mol. Med.* **2004**, *8*, 294-300.
51
52
53 60. Marçola, M.; Rodrigues, C. E. Endothelial progenitor cells in tumor angiogenesis:
54
55 another brick in the wall. *Stem Cells Int.* **2015**, *2015*, 832649.
56
57
58
59
60

- 1
2
3
4
5
6
7
8
9
10
11
12
13
14
15
16
17
18
19
20
21
22
23
24
25
26
27
28
29
30
31
32
33
34
35
36
37
38
39
40
41
42
43
44
45
46
47
48
49
50
51
52
53
54
55
56
57
58
59
60
61. The expression of β_1 integrins (e.g. $\alpha_5\beta_1$) in EPCs was also evaluated; it was determined to be about 35-40%, lower than the expression of $\alpha_v\beta_3$ (>87.5%).
62. Chen, P. Y.; Qin, L.; Zhuang, Z. W.; Tellides, G.; Lax, I.; Schlessinger, J.; Simons, M. The docking protein FRS2 α is a critical regulator of VEGF receptors signaling. *Proc. Natl. Acad. Sci. U. S. A.* **2014**, *111*, 5514-5519.
63. Margheri, F.; Killa, A.; Laurenzana, A.; Serrati, S.; Mazzanti, B.; Saccardi, R.; Santosuosso, M.; Danza, G.; Sturli, N.; Rosati, F.; Magnelli, L.; Papucci, L.; Calorini, L.; Bianchini, F.; Del, R. M.; Fibbi, G. Endothelial progenitor cell-dependent angiogenesis requires localization of the full-length form of uPAR in caveolae. *Blood* **2011**, *118*, 3743-3755.
64. Carmi, C.; Galvani, E.; Vacondio, F.; Rivara, S.; Lodola, A.; Russo, S.; Aiello, S.; Bordi, F.; Costantino, G.; Cavazzoni, A.; Alfieri, R.R.; Ardizzoni, A.; Petronini, P. G.; Mor, M. Irreversible inhibition of epidermal growth factor receptor activity by 3-aminopropanamides. *J. Med. Chem.* **2012**, *55*, 2251-2264.
65. Olive, D. M. Quantitative methods for the analysis of protein phosphorylation in drug development. *Expert Rev. Proteomics* **2004**, *1*, 327-341.
66. CEREP, catalogue on line:
http://www.cerep.fr/cerep/users/pages/catalog/Affiche_CondExp_Test.asp?test=2900 (for PDGFR β , November 29, 2016) and
http://www.cerep.fr/cerep/users/pages/catalog/Affiche_CondExp_Test.asp?test=2864 (for VEGFR2, November 29, 2016).

Table of Contents Graphic

